

Received August 29, 2019, accepted September 20, 2019, date of publication September 24, 2019, date of current version October 7, 2019.

Digital Object Identifier 10.1109/ACCESS.2019.2943480

# Multi-Objective Optimal Power Flow Based on Hybrid Firefly-Bat Algorithm and Constraints-Prior Object-Fuzzy Sorting Strategy

GONGGUI CHEN<sup>1,2</sup>, JIE QIAN<sup>1,2</sup>, ZHIZHONG ZHANG<sup>3</sup>, AND ZHI SUN<sup>4</sup>

<sup>1</sup>Key Laboratory of Industrial Internet of Things & Networked Control, Ministry of Education, Chongqing University of Posts and Telecommunications, Chongqing 400065, China

<sup>2</sup>Chongqing Key Laboratory of Complex Systems and Bionic Control, Chongqing University of Posts and Telecommunications, Chongqing 400065, China

<sup>3</sup>Key Laboratory of Communication Network and Testing Technology, Chongqing University of Posts and Telecommunications, Chongqing 400065, China

<sup>4</sup>Chn Energy Enshi Hydropower Company Ltd., Enshi 445000, China

Corresponding author: Zhizhong Zhang (zhangztx@163.com)

This work was supported by the National Natural Science Foundation of China under Grant 51207064 and Grant 61463014.

**ABSTRACT** In this paper, a novel hybrid firefly-bat algorithm with constraints-prior object-fuzzy sorting strategy (HFBA-COFS) is put forward to solve the strictly-constrained multi-objective optimal power flow (MOOPF) problems. The hybrid firefly-bat algorithm (HFBA) integrates the dimension-based firefly algorithm and the modified bat algorithm to improve the population-diversity and global-exploration ability of original algorithm. To handle the unqualified state variables and overcome the deficiency of traditional penalty function approach (PFA), the constraints-prior Pareto-dominant rule (CPR) which takes constraints-violation and objectives-value into consideration is proposed in this paper. Furthermore, an effective constraints-prior object-fuzzy sorting (COFS) strategy based on CPR rule is presented to seek the well-distributed Pareto optimal set (POS) in solving the MOOPF problems. To validate the great advantages of HFBA-COFS algorithm, ten MOOPF cases optimizing active power loss, total emission and fuel cost are simulated on the IEEE 30-bus, IEEE 57-bus and IEEE 118-bus systems. In addition, the generational distance and SPREAD evaluation indexes powerfully demonstrate that the proposed HFBA-COFS algorithm can achieve high-quality POS, which has great significance to realize the safe and economic operation of large-scale power systems.

**INDEX TERMS** Hybrid firefly-bat algorithm, constraints-prior object-fuzzy sorting strategy, multi-objective optimal power flow problem, economic operation.

## I. INTRODUCTION


The optimal power flow (OPF), as a predominant tool to realize the economic and stable operation of electrical systems, is very vital for the enhancement of power quality. In general, the OPF problem primarily aims to achieve the minimal fuel cost or active power loss by adjusting the independent variables of power systems [1]–[4].

Recently, the multi-objective optimal power flow (MOOPF) problems, which can evaluate the running status of power systems more comprehensively, have attracted extensive attention. In essence, the MOOPF problem is a minimum optimization with multiple contradictory objectives and strict

constraints [5]–[8]. Unlike the OPF problem determining the only optimal solution, solving the MOOPF problems focuses on seeking a high-quality Pareto optimal set (POS) on the premise of satisfying various constraints. The non-convex and non-differentiable characteristics of MOOPF problems make it difficult to be solved by traditional methods.

### A. METHOD REVIEW AND ALGORITHM SELECTION

The maturity of computer technology makes it possible to solve the MOOPF problems by intelligent algorithms. At present, the meta-heuristic algorithm [9], the improved strength Pareto evolutionary algorithm [10], the modified bio-inspired algorithm [11], and the multi-objective dimension-based firefly algorithm [12] are all effective to handle the MOOPF problems. However, it is a pity that the common

The associate editor coordinating the review of this manuscript and approving it for publication was Ton Do .

algorithms cannot deal well with the tri-objective MOOPF problems or the bi-objective ones of large-scale power systems such as the IEEE 57-bus or 118-bus systems.

The original and modified bat algorithms with superior accuracy and fewer parameters have been applied to many practical fields such as the wireless sensor network deployment [13] and the low-carbon job shop scheduling problem [14]. Besides, the extensive applicability of bat algorithm makes it suitable to solve the economic dispatch and optimal power flow problems [15]–[17]. Therefore, the bat algorithm is chosen to handle the MOOPF problems in this paper and several improvements are adopted to overcome the defect of standard algorithm.

## B. CONTRIBUTIONS

To realize the safe and economical operation of power system, a hybrid firefly-bat algorithm with constraints-prior object-fuzzy sorting strategy (HFBA-COFS) is proposed to solve the MOOPF problems. Simulation results clearly state that the HFBA-COFS algorithm has incomparable advantages over other published methods in dealing with the many-objective optimizations of large-scale power systems. The main contributions of this paper are listed as follows.

### 1) HFBA ALGORITHM

First, the hybrid firefly-bat algorithm (HFBA) which can avoid premature-convergence and optimize solution-diversity is proposed. The HFBA algorithm which is effective to solve the non-linear MOOPF problems has been modified from the following two aspects.

#### a: INITIAL POPULATION OPTIMIZATION

The initial population of HFBA algorithm is determined by the multi-objective dimension-based firefly algorithm (MODFA). The great superiority of MODFA algorithm in handling MOOPF problems can refer to literature [12]. The preliminary screening of power flow solutions based on MODFA algorithm will increase the probability and efficiency of HFBA algorithm in finding the more preferable POS sets.

#### b: PARAMETER UPDATING OPTIMIZATION

Besides, expanding population-diversity helps to explore the higher-performance POS set. Based on this, a nonlinear weight coefficient is incorporated into the velocity term of basic bat algorithm and a monotone random filling model (MRFM) is put forward to modify the update mode of two local parameters.

### 2) COFS SORTING STRATEGY

Furthermore, a constraints-prior object-fuzzy sorting strategy (COFS) is proposed in this paper to seek the uniformly-distributed POS without any constraint-violation. The suggested COFS sorting rule, which has great superiorities in solving the multi-dimensional MOOPF problems, comprehensively takes the *Rank* index based on objective values

and the fuzzy dominant fitness (*Fudf*) index based on control variables into account.

Finally, combining the HFBA algorithm and COFS sorting strategy, the novel HFBA-COFS algorithm is put forward in this paper. In contrast to the typical non-dominated sorting genetic algorithm-II (NSGA-II) and DE-PFA algorithms, the applicability and superiority of presented HFBA-COFS algorithm in solving the strictly-constrained MOOPF problems are validated. It should be noted that the DE-PFA algorithm is the integration of multi-objective differential evolution algorithm (MODE) and penalty function approach (PFA). Compared with the NSGA-II method, which is often used as a benchmark for the performance evaluation of many-objective algorithm, the advantages of the novel HFBA-COFS algorithm can be fully and reasonably proved.

The rest of this paper is constructed as follows. The mathematic model of MOOPF problems including four objective functions, multiple equality and inequality constraints is presented in Section II. Section III introduces the involved multi-objective strategies including the constraint handling strategies and the non-inferior sorting strategy. Section IV focuses on the proposed HFBA-COFS algorithm and its application on the MOOPF problems. The numerous results of ten MOOPF trials simulated on three different-scale systems are presented in Section V. To verify the availability and superiority of HFBA-COFS algorithm, Section VI gives a comprehensive analysis of experiment results mainly based on the dominance rate, performance metrics and computational complexity. In the end, the conclusion is given in Section VII.

## II. MATHEMATICAL MODEL

For mathematical model of MOOPF problems, the four objective functions and two types of system restrictions are introduced as follows.

### A. OBJECTIVES

The four objectives, known as total emission  $Ob_e$ , basic fuel cost  $Ob_f$ , fuel cost with value-point loadings  $Ob_{fv}$ , and active power loss  $Ob_p$ , are studied in this paper.

#### 1) TOTAL EMISSION

$$Ob_e = \sum_{i=1}^{N_G} [\alpha_i P_{Gi}^2 + \beta_i P_{Gi} + \gamma_i + \eta_i \exp(\lambda_i P_{Gi})] \text{ton/h} \quad (1)$$

where  $N_G$  is the amount of generators and  $P_{Gi}$  represents the active power of the  $i$ th generator node. The  $\alpha_i$ ,  $\beta_i$ ,  $\gamma_i$ ,  $\eta_i$  and  $\lambda_i$  are emission coefficients of the  $i$ th generator.

#### 2) BASIC FUEL COST

$$Ob_f = \sum_{i=1}^{N_G} (a_i + b_i P_{Gi} + c_i P_{Gi}^2) \$/h \quad (2)$$

where  $a_i$ ,  $b_i$  and  $c_i$  depict the cost coefficients of the  $i$ th generator.

3) FUEL COST CONSIDERING VALUE-POINT EFFECT

$$Ob_{fv} = \sum_{i=1}^{N_G} (a_i + b_i P_{Gi} + c_i P_{Gi}^2 + |d_i \times \sin(e_i \times (P_{Gi}^{\min} - P_{Gi}))|) \$/h \quad (3)$$

where  $d_i$  and  $e_i$  are two coefficients of valve-point effect.

4) ACTIVE POWER LOSS

$$Ob_p = \sum_{k=1}^{N_L} con(k) [V_i^2 + V_j^2 - 2V_i V_j \cos(\delta_i - \delta_j)] MW \quad (4)$$

where  $V_i$  and  $\delta_i$  represent the voltage magnitude and angle of the  $i$ th bus. The  $N_L$  is the amount of transmission lines and  $con(k)$  indicates the conductance of the  $k$ th branch that links the  $i$ th bus to the  $j$ th one.

**B. RESTRICTIONS**

The system constraints are divided into equality constraints and the inequality ones.

1) EQUALITY RESTRICTIONS

The equality constraints defined as (5) and (6) virtually reveal the power balance of electric systems.

$$P_{Gi} - P_{Di} - V_i \sum_{j \in N_i} V_j (G_{ij} \cos \delta_{ij} + B_{ij} \sin \delta_{ij}) = 0, \quad i \in N \quad (5)$$

$$Q_{Gi} - Q_{Di} - V_i \sum_{j \in N_i} V_j (G_{ij} \sin(\delta_i - \delta_j) - B_{ij} \cos(\delta_i - \delta_j)) = 0, \quad i \in N_{PQ} \quad (6)$$

where  $N_i$ ,  $N$  and  $N_{PQ}$  are the numbers of the nodes linked to the  $i$ th node, the nodes except the slack one and the PQ nodes. The definitions of other mentioned parameters are clarified in literatures [7], [12], [18].

2) INEQUALITY RESTRICTIONS

The inequality constraints include the restrictions on state variables which are defined as (7)~(10) and the restrictions on control variables which are described as (11)~(14).

- ▶ active power at slack bus  $P_{G1}$

$$P_{G1}^{\max} \geq P_{G1} \geq P_{G1}^{\min} \quad (7)$$

- ▶ voltage at load bus  $V_L$

$$V_{Li}^{\max} \geq V_{Li} \geq V_{Li}^{\min}, \quad i \in N_{PQ} \quad (8)$$

- ▶ reactive power at generator bus  $Q_G$

$$Q_{Gi}^{\max} \geq Q_{Gi} \geq Q_{Gi}^{\min}, \quad i \in N_G \quad (9)$$

- ▶ apparent power  $S$

$$S_i^{\max} - S_i \geq 0, \quad i \in N_L \quad (10)$$

- ▶ generator active power  $P_G$

$$P_{Gi}^{\max} \geq P_{Gi} \geq P_{Gi}^{\min}, \quad i = 2, 3, \dots, N_G \quad (11)$$

- ▶ voltage at generator bus  $V_G$

$$V_{Gi}^{\max} \geq V_{Gi} \geq V_{Gi}^{\min}, \quad i \in N_G \quad (12)$$

- ▶ transformer tap-settings  $T$

$$T_i^{\max} \geq T_i \geq T_i^{\min}, \quad i \in N_T \quad (13)$$

- ▶ reactive power injection  $Q_C$

$$Q_{Ci}^{\max} \geq Q_{Ci} \geq Q_{Ci}^{\min}, \quad i \in N_C \quad (14)$$

where  $N_C$  and  $N_T$  indicate the numbers of shunt compensators and transformers.

**III. MULTI-OBJECTIVE STRATEGIES**

Then, the constraint handling measures, the non-inferior dominant and sorting strategies are clarified.

**A. CONSTRAINT HANDLING STRATEGIES**

The power flow optimal solution adopted by decision makers should meet all constraints of electric system. As the ending condition of Newton-Raphson approach, the equality constraints (5) and (6) can be satisfied at the end of calculation process. The handling strategies of inequality restrictions are mainly discussed in this paper.

1) CONTROL VARIABLES PROCESSING

The  $D$ -dimensional control variables  $C$ , also the independent variables of power system, are limited within  $[C^{\min}, C^{\max}]$ . The  $C$  set which violates inequality constraints can be adjusted as (15).

$$C_i = \begin{cases} C_i^{\min}, & C_i < C_i^{\min} \\ C_i^{\max}, & C_i > C_i^{\max} \end{cases} \quad (15)$$

2) STATE VARIABLES PROCESSING

The common PFA method deals with the state variables  $S$  which violate inequality constraints by introducing multiple penalty coefficients, which has obvious limitations.

*a: PENALTY FUNCTION APPROACH*

Based on PFA method, the objective functions are modified as follows.

$$Ob_{obj-mod} = Ob_{obj} + Penalty \quad (16)$$

$$Penalty = \zeta_P (P_{G1} - P_{G1}^{\lim}) + \zeta_V \sum_{i=1}^{N_{PQ}} (V_{Li} - V_{Li}^{\lim}) + \zeta_Q \sum_{i=1}^{N_G} (Q_{Gi} - Q_{Gi}^{\lim}) + \zeta_S \sum_{i=1}^{N_L} (S_i - S_i^{\lim}) \quad (17)$$

$$\zeta_{(ite)^k} = \zeta^{\min} + ite^k (\zeta^{\max} - \zeta^{\min}) / ite^{\max} \quad (18)$$

where  $\zeta_P$ ,  $\zeta_V$ ,  $\zeta_Q$  and  $\zeta_S$  are penalty coefficients which are adjusted as formula (18) during the iterations. The  $\zeta_{(ite^k)}$  is the penalty coefficient value at the  $k$ th iteration and  $ite^{max}$  indicates the maximum iteration number. The corresponding penalty coefficients are limited within  $[\zeta^{min}, \zeta^{max}]$ .

The specific application of PFA method can be referred to literatures [19]–[21]. Proverbially, the performance of PFA method is closely related to the appropriateness of penalty coefficients. However, determining a proper penalty coefficient requires plentiful repeated experiments and it is hard to guarantee that every solution of obtained POS satisfies all constraints, especially on large-scale systems. To overcome the shortcomings of PFA method, a constraints-prior dominant rule (CPR) is proposed.

#### b: CPR DOMINANT RULE

The CPR rule defines the dominant relationship of two different power flow solutions by calculating the values of objectives and the violations of inequality constraints. In detail, the judgment can be made that the  $So_1$  ( $So_1 = (u_1, u_2, \dots, u_D)$ ) solution dominates the  $So_2$  ( $So_2 = (v_1, v_2, \dots, v_D)$ ) one when condition (19) or (20) is met.

$$Vio(So_1) < Vio(So_2) \quad (19)$$

$$\begin{cases} Vio(So_1) = Vio(So_2) \\ Ob_i(C, S_1) \leq Ob_i(C, S_2), \forall i \in \{1, 2, \dots, M\} \\ Ob_j(C, S_1) < Ob_j(C, S_2), \exists j \in \{1, 2, \dots, M\} \end{cases} \quad (20)$$

where  $Vio(So_m)$  represents the total violation value of the  $m$ th solution. The  $Ob_i(C, S_n)$  indicates the  $i$ th objective value of the  $n$ th  $S$  set and  $M$  ( $M \geq 2$ ) is the number of simultaneous optimization goals.

The suggested CPR method can effectively avoid the complicated process of selecting appropriate coefficients by PFA method.

#### B. COFS SORTING STRATEGY

Based on the presented CPR method, an innovative COFS strategy to seek the well-distributed Pareto fronts (PFs) is put forward in this paper. The COFS strategy comprehensively considers the *Rank* index achieved by CPR method and the *Fudf* index calculated based on control variables.

##### 1) RANK INDEX

Learning from the typical non-inferior sorting rule proposed by Kalyanmoy Deb [22]–[24], the *Rank* indicator of each solution can be determined as follows.

a) Generate a candidate population (*CAP*) by integrating the paternal population (*PAP*) and the elite population (*ELP*). The initial *PAP* and *ELP* populations are composed by  $T$  randomly generated individuals.

b) Calculate the *Ob* and *Vio* values of each individual in *CAP* population.

c) Based on the suggested CPR method, these power flow solutions, which are not dominated by other solutions in *CAP* population, are assigned as *Rank* = 1.

d) Eliminate the individuals with *Rank* = 1. The current non-inferior solutions are found and assigned as *Rank* = 2 according to the same CPR rule.

e) The above operations are repeated until each solution in *CAP* population has been assigned a corresponding *Rank* index.

##### 2) FUDF INDEX

The *Fudf* index is used to judge the dominant relation of two individuals with the same *Rank* index. In detail, the *Fudf* index of each solution can be calculated as follows.

a) Compute the relative performance of the  $So_1$  solution in contrast to the  $So_2$  one ( $P_{uv}(So_1)$ ) as formula (21).

$$P_{uv}(So_1) = So_1 - So_2 = (u_1 - v_1, u_2 - v_2, \dots, u_D - v_D) \quad (21)$$

b) Based on the fuzzy membership function  $F_m$  defined as (22), the dominant degree of  $So_1$  solution relative to the  $So_2$  one ( $\varphi(So_1)$ ) is determined according to formula (23).

$$F_m = \begin{cases} 1, & x \leq -1 \\ \chi_1 x^3 + \chi_2, & -1 < x < 1 \quad \chi_1 = -0.5, \chi_2 = -\chi_1 \\ 0, & x \geq 1 \end{cases} \quad (22)$$

$$\varphi(So_1) = F_m(P_{uv}(So_1)) = (\varphi_1^u, \dots, \varphi_D^u) \quad (23)$$

c) Calculate the fuzzy eigenvalue of  $So_1$  solution ( $\psi(So_1)$ ) based on formula (24).

$$\psi(So_1) = \prod_i \varphi_i^u (i \in [1, D]) \cap (\varphi_i^u \neq 0) \quad (24)$$

d) Clarify the standard performance of  $So_1$  solution relative to the  $So_2$  one named as  $SP_{uv}(So_1)$  according to (25).

$$SP_{uv}(So_1) = \psi(So_1) / (\psi(So_1) + \psi(So_2)) \quad (25)$$

The  $Fudf(So_i)$ , the mean value of standard performances in essential, represents the Pareto fuzzy dominant fitness of the  $i$ th solution relative to the other ( $2T-1$ ) solutions of *CAP* population. The  $Fudf(So_i)$  character can be calculated as formula (26).

$$Fudf(So_i) = \sum_j^j SP / (2T - 1, j = 1, 2, \dots, 2T \cap j \neq i) \quad (26)$$

The core steps to judge the adoption-priority of each power flow solution based on the proposed COFS strategy can be summarized as follows. More concretely, the  $So_1$  solution has a higher adoption-priority than the  $So_2$  one when condition (27) or (28) is satisfied.

$$Rank(So_1) < Rank(So_2) \quad (27)$$

$$\begin{cases} Rank(So_1) = Rank(So_2) \\ Fudf(So_1) > Fudf(So_2) \end{cases} \quad (28)$$

Generally, the  $T$  top-ranked solutions in *CAP* population are the ultimate POS selected by the COFS sorting strategy.

#### IV. OPTIMIZATION ALGORITHMS

The basic bat algorithm is popular for its high-accuracy and good-versatility. To release the restriction of local optimums and improve searching efficiency, the improved HFBA-COFS algorithm is proposed.

##### A. STANDARD BAT ALGORITHM

The standard bat algorithm, as a classical global optimization algorithm, updates the location of bat population by constantly adjusting searching frequency and determines the global optimal individual according to the established dominant relationship [25]–[27]. The frequency  $Fr(i)$ , speed  $Sp(i)$  and location  $Lo(i)$  of the  $i$ th bat are defined as (29), (30) and (31).

$$Fr(i) = Fr^{\min} + \tau_1 * (Fr^{\max} - Fr^{\min}) \quad (29)$$

$$Sp(i)_{(t)} = Sp(i)_{(t-1)} + Fr(i) * (Lo(i)_{(t-1)} - Lo_{best}) \quad (30)$$

$$Lo(i)_{(t)} = Lo(i)_{(t-1)} + Sp(i)_{(t)} \quad (31)$$

where the frequency is restricted within  $[Fr^{\min}, Fr^{\max}]$ . The  $\tau_1$  ( $\tau_1 \in (0,1)$ ) is a random number and  $Lo_{best}$  indicates the location of the current best individual.

Local searching operation, as the unique feature of bat algorithm, is mainly to explore a preferable individual ( $Lo_{new}$ ) near the  $Lo_{best}$  one. Two principal parameters of local searching, known as the loudness  $lou$  and pulse rate  $pul$ , are described as (32) and (33), respectively.

When  $lou$  and  $pul$  meet the preset conditions, the local search which is conducive to optimize the diversity of bat population will be performed based on formula (34).

$$lou(i)_{(t+1)} = \tau_2 * lou(i)_{(t)} \quad (32)$$

$$pul(i)_{(t+1)} = pul_0(1 - \exp(-\xi_1 t)) \quad (33)$$

$$Lo_{new} = Lo_{best} + \tau_3 * Lo_{best} \quad (34)$$

where  $\tau_2$  ( $\tau_2 \in (0,1)$ ) and  $\tau_3$  ( $\tau_3 \in (-1,1)$ ) are two random numbers. The  $\xi_1$  ( $\xi_1 > 0$ ) represents the attenuation coefficient of  $lou$  while  $pul_0$  indicates the initial pulse rate.

##### B. PROPOSED HFBA-COFS ALGORITHM

In order to handle the MOOPF problems more effectively, the HFBA algorithm is born by the following improvements to the standard algorithm.

###### 1) MODIFIED MANNER OF SPEED

The non-linear weight coefficient  $\omega_{non}$  defined as (35) is employed to improve the updating manner of  $Sp$ . The modified manner of  $Sp$  is described as (36).

$$\begin{aligned} \omega_{non}(t) = & \omega_{non}^{\max} - \tau_4(\omega_{non}^{\max} - \omega_{non}^{\min}) \\ & + \tau_5(\omega_{non}(t-1) - 0.5 * (\omega_{non}^{\max} + \omega_{non}^{\min})) \end{aligned} \quad (35)$$

$$Sp(i)_{(t+1)} = \omega_{non}(t)Sp(i)_{(t)} + \tau_6 Fr(i)(Lo_{best} - Lo(i)_{(t)}) \quad (36)$$

where  $\omega_{non}$  is limited within  $[\omega_{non}^{\min}, \omega_{non}^{\max}]$  and  $\tau_i$  ( $\tau_i \in (0,1)$ ,  $i = 4,5,6$ ) are three random numbers.

###### 2) MODIFIED MANNER OF LOCAL SEARCHING

The MRFM model, which is put forward to improve the updating manners of two local parameters, can meet the specific requirements of smaller  $lou$  and larger  $pul$  when the  $Lo_{new}$  individual is accepted. The renewed manners of  $lou$  and  $pul$  are defined as (37) and (38), respectively.

$$lou_{new}(i) = \frac{(lou^{\max} - lou^{\min}) * (ite - ite_{max})}{(1 - ite_{max})} + lou^{\min} \quad (37)$$

$$pul_{new}(i) = \frac{(pul^{\min} - pul^{\max}) * (ite - ite_{max})}{(1 - ite_{max})} + pul^{\max} \quad (38)$$

The MRFM model sets the valid range of loudness to  $[lou^{\min}, lou^{\max}]$  and the effective range of pulse rate to  $[pul^{\min}, pul^{\max}]$ . The  $ite$  and  $ite_{max}$  indicate the current and maximum iteration numbers.

The modified manner of local searching is summarized as Figure 1.

###### 3) MODIFIED MANNER OF POPULATION INITIALIZATION

For the researches on MOOPF problems, the typical method of generating an initial population is shown as (39). However, this randomly-generated way will inevitably increase searching time to determine the optimal solutions. Therefore, this paper proposes the creative idea of adopting the MODFA algorithm for preliminary optimization, and takes the obtained POS (POS<sub>-FA</sub>) as the initial  $PAP$  population of HFBA-COFS algorithm. The applications of firefly algorithm can be found in literatures [12], [28]–[30].

$$C(i) = C_i^{\min} + \tau_7 (C_i^{\max} - C_i^{\min}) i \in [1, T] \quad (39)$$

where  $C(i)$  represents the  $i$ th initial control variables set and  $\tau_7$  ( $\tau_7 \in (0,1)$ ) is a random number.

By integrating the above improvements and suggested COFS strategy, the HFBA-COFS algorithm which provides an effective way to solve the MOOPF problems is proposed. Besides, Table 1 summarizes the pseudo-codes of HFBA-COFS algorithm for handling the MOOPF problems.

#### V. SIMULATION TRIALS

There are ten cases simulated on three different-scale power systems. Comparing with the DE-PFA and NSGA-II algorithms, the definite superiorities of HFBA-COFS algorithm in solving the bi-objective and tri-objective MOOPF problems can be proved.

##### A. SYSTEMS AND OBJECTIVE COMBINATIONS

The IEEE 30-bus, IEEE 57-bus and the more complex IEEE 118-bus systems are employed to simulate the mentioned MOOPF trials shown in Table 2. All trials are carried out on the MATLAB 2014a software in a PC with Intel(R) Core(TM) i5-7500 CPU @ 3.40 GHz with 8GB RAM.

The transformer taps of the IEEE 30-bus system, which includes 6 generators and 24-dimensional control variables,

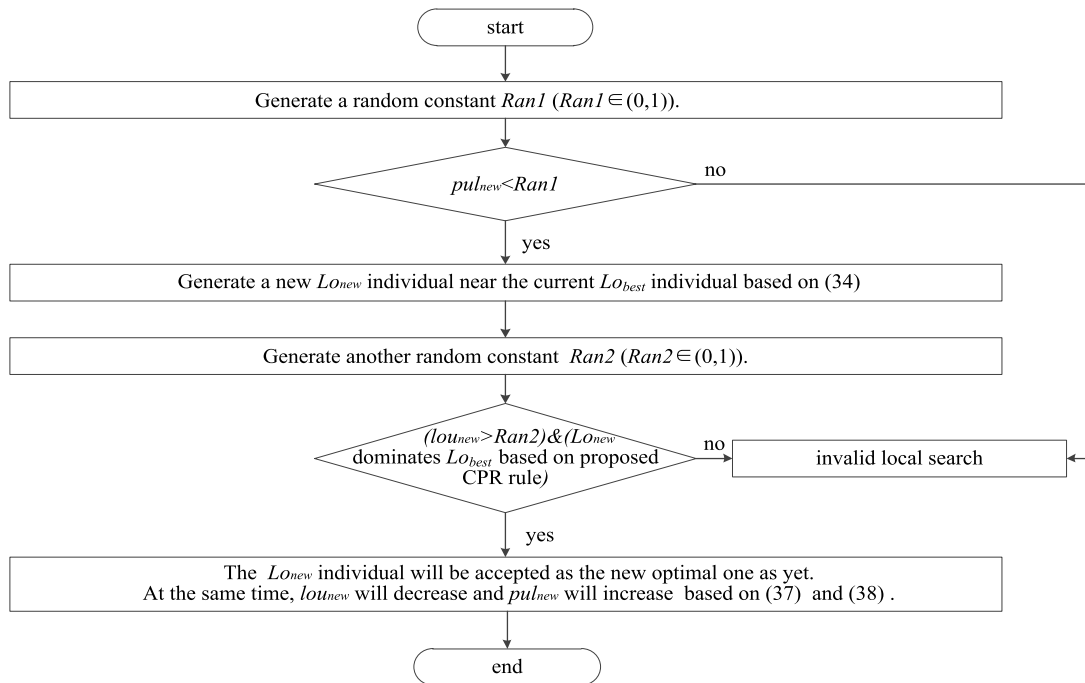


FIGURE 1. Local search of HFBA-COFS algorithm.

TABLE 1. Pseudo codes of HFBA-COFS algorithm on MOOPF problems.

**input:** the initial parameters of HFBA-COFS algorithm

**begin**

$ite_{FA}=1$

Based on formula (39), the initial population is generated as the input of MODFA algorithm.

**while**  $ite_{FA} < ite_{FA-max}$

Determine the  $POS_{FA}$  set obtained by the MODFA method shown in literature [12].

$ite_{FA} = ite_{FA} + 1$ ;

**end while**

$ite=1$

Take the obtained  $POS_{FA}$  set as the initial  $PAP$  population.

**while**  $ite < ite_{max}$

**for**  $i=1,2,\dots,T$

Update the  $Sp(i)$  and  $Lo(i)$  of  $i$ th individual based on (36) and (31).

Clarify the values of  $Ob_i$  and  $Vio(i)$  by calculating power flow.

**end**

Determine the current POS set based on the presented COFS sorting strategy.

Determine the  $LO_{best}$  solution based on the fuzzy affiliation method shown in literature [12].

Perform the local search around the  $LO_{best}$  solution shown in Figure 1 to generate the  $LO_{new}$  solution.

**if** the  $LO_{new}$  solution dominates the  $LO_{best}$  one according to the suggested CPR rule

$LO_{best} = LO_{new}$

**end**

$ite=ite+1$ ;

**end while**

**end**

**output:** the ultimate POS set of HFBA-COFS algorithm and the control variables set of the  $LO_{best}$  solution

are limited within [0.9 1.1] p.u.. The voltage limits of generator nodes are restricted within [0.95 1.1] p.u.. The fuel cost and emission coefficients of IEEE 30-bus system are given in Table 3. The structure and more details of IEEE 30-bus system can be found in literatures [7], [12], [31], [32].

The transformer taps of the IEEE 57-bus system, which includes 33-dimensional control variables, are limited within

[0.9 1.1] p.u.. The shunt capacitor is limited within [0 0.3] p.u. while the voltage magnitude of PQ and PV nodes are limited in [0.9 1.1] p.u.. The structure and more details such as emission coefficients of IEEE 57-bus system are obtained from literatures [7], [33].

As a representative large-scale power system, the IEEE 118-bus system with 128-dimensional control variables can

TABLE 2. Objective combinations.

objective	case1	case2	case3	case4	case5	case6	case7	case8	case9	case10
$Ob_e$	yes			yes	yes	yes	yes			yes
$Ob_f$	yes	yes		yes		yes	yes	yes	yes	yes
$Ob_{fv}$			yes		yes					
$Ob_p$		yes	yes	yes	yes		yes	yes	yes	yes
system	IEEE30	IEEE30	IEEE30	IEEE30	IEEE30	IEEE57	IEEE57	IEEE57	IEEE118	IEEE118

TABLE 3. Fuel cost and emission coefficients of IEEE 30-bus system.

		Emission coefficients					Fuel cost coefficients				
		$\alpha$	$\beta$	$\gamma$	$\eta$	$\lambda$	$a$	$b$	$c$	$d$	$e$
Generator	$G_1$	0.06490	-0.05554	0.04091	0.0002	2.857	0	2	0.00375	18	0.037
	$G_2$	0.05638	-0.06047	0.02543	0.0005	3.333	0	1.75	0.0175	16	0.038
	$G_5$	0.04586	-0.05094	0.04258	0.000001	8.000	0	1	0.0625	14	0.04
	$G_8$	0.0338	-0.0355	0.05326	0.002	2.000	0	3.25	0.00834	12	0.045
	$G_{11}$	0.04586	-0.05094	0.04258	0.000001	8.000	0	3	0.025	13	0.042
	$G_{13}$	0.05151	-0.05555	0.06131	0.00001	6.667	0	3	0.025	13.5	0.041

measure the performance of HFBA-COFS algorithm more comprehensively. The structure and more details of IEEE 118-bus system can be found in literatures [7], [12].

**B. ALGORITHM PARAMETERS SETTING**

To determine a relatively optimal parameters set of HFBA-COFS algorithm, a bi-objective case which optimizes the  $Ob_e$  and  $Ob_f$  at the same time is adopted as an example. The two local parameters have great influences on optimization performance and their proper ranges are studied. Figure 2 gives the PFs with different *pul* ranges and it shows the range of [0.09 0.51] obtains the worst PF while the range of [0.10 0.50] achieves the best one. Figure 3 gives the PFs with different *lou* ranges and it clearly indicates that the range of [0.50 0.96] achieves the best PF with evenly-distribution. Therefore, the appropriate ranges of pulse rate and loudness are set as [0.10 0.50] and [0.50 0.96] in this paper. The other detail parameter-settings are summarized in Table 4.

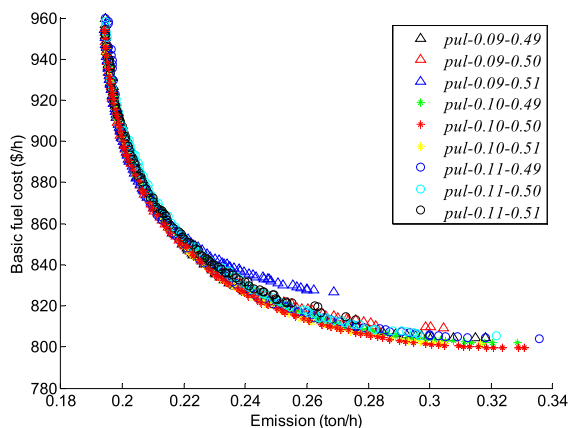


FIGURE 2. PFs with different *pul* ranges.

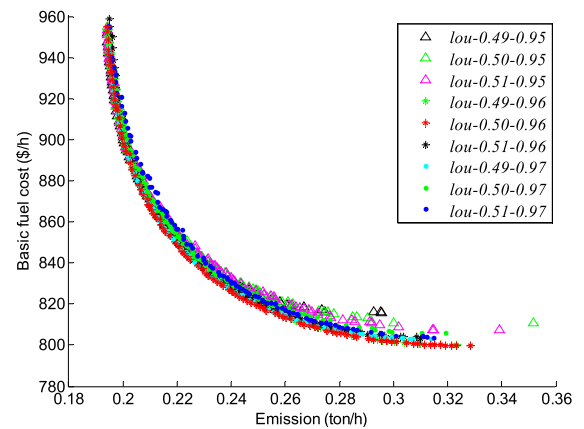


FIGURE 3. PFs with different *lou* ranges.

**C. TRIALS ON IEEE 30-BUS SYSTEM**

Three bi-objective and two tri-objective MOOPF trials are carried out on the IEEE 30-bus system.

1) CASE1:  $Ob_E$  and  $Ob_f$

An optimization case which aims at minimizing the emission and basic fuel cost simultaneously is implemented on the IEEE 30-bus system. The PFs of case1 found by DE-PFA, NSGA-II and proposed HFBA-COFS algorithms are shown in Figure 4. The best compromise solution (BCS) of each algorithm is also noted in Figure 4. It intuitively shows the PF obtained by HFBA-COFS algorithm is better than these of DE-PFA and NSGA-II methods. At the same time, the numbers of feasible solutions obtained by three algorithms are shown in Figure 5. It is worth noting that the feasible solution in this paper represents the non-inferior solution which does not violate any equality or inequality constraints. Figure 5 clearly indicates the all Pareto solutions determined

TABLE 4. Parameter-settings of three involved algorithms.

parameters	case1~case5			case6~case10		
	DE-PFA	NSGA-II	HFBA-COFS	DE-PFA	NSGA-II	HFBA-COFS
$T$	100	100	100	100	100	100
$ite_{FA-max}$	-	-	50	-	-	100
$ite_{max}$	300	300	150	500	500	300
$\zeta^{min}/\zeta^{max}$	10/100	-	-	10/100	-	-
mutant coefficient	0.6	-	-	0.6	-	-
crossover coefficient	0.8	-	-	0.8	-	-
mutation index/percentage	-	20/1	-	-	20/1	-
crossover index/percentage	-	20/0.1	-	-	20/0.1	-
light absorption coefficient	-	-	1	-	-	1
randomization parameter	-	-	0.1	-	-	0.1
attractiveness at distance=0	-	-	1	-	-	1
$\omega_{best}^{min}/\omega_{non}^{max}$	-	-	0.4/0.9	-	-	0.4/0.9
$Fp^{min}/Fp^{max}$	-	-	0/2	-	-	0/2
$pu^{min}/pu^{max}$	-	-	0.10/0.50	-	-	0.10/0.50
$lou^{min}/lou^{max}$	-	-	0.50/0.96	-	-	0.50/0.96

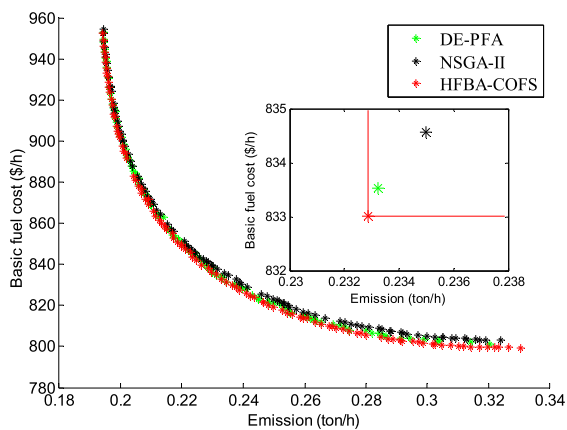


FIGURE 4. PFs of case1.

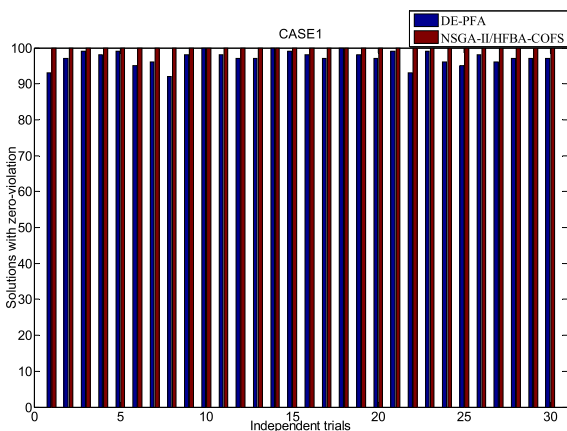


FIGURE 5. The numbers of feasible solutions for case1.

by NSGA-II and HFBA-COFS algorithms achieve zero constraints-violation. It powerfully demonstrates that the presented COFS sorting strategy effectively overcomes the shortcomings of PFA method.

In addition, Table 5 gives the control variables of BCS solutions for case1. Adjusting the input of electronic devices

based on the control variables can make the power system achieve the predetermined economic operating state, which is the practical significance of studying the MOOPF problems. According to the objective values, the BCS of HFBA-COFS algorithm with 0.2329 ton/h of  $Ob_e$  and 833.0155 \$/h of  $Ob_f$  dominates the BCS solutions of DE-PFA and NSGA-II methods.

Moreover, Table 6 gives the comparison results of BCS solutions from other published literatures and provides more convincing proofs for the superiority of HFBA-COFS algorithm.

### 2) CASE2: $OB_p$ and $Ob_f$

In case2, the power loss and the basic fuel cost are optimized at the same time. The PFs of case2 obtained by three involved algorithms are given in Figure 6. It indicates that the suggested HFBA-COFS algorithm can achieve the best PF with uniformly-distribution while the NSGA-II method obtains the worst one. Figure 7 gives the numbers of feasible solutions for case2 which clearly demonstrates the obvious advantages of HFBA-COFS algorithm in seeking more zero-violation

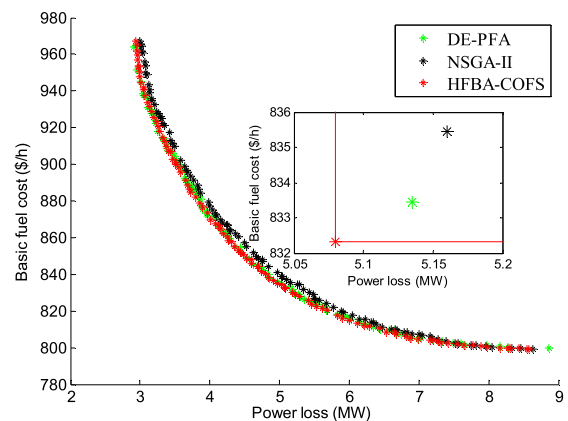


FIGURE 6. PFs of case2.



TABLE 5. The control variables of BCS for case1 and case2.

variables	case1			case2		
	DE-PFA	NSGA-II	HFBA-COFS	DE-PFA	NSGA-II	HFBA-COFS
$P_{G2}$ (MW)	57.2272	56.9089	57.9934	49.9374	52.2694	53.1358
$P_{G5}$ (MW)	26.9386	25.1412	28.4303	32.8074	33.5875	32.4210
$P_{G8}$ (MW)	35.0000	34.8792	32.9613	32.9055	35.0000	35.0000
$P_{G11}$ (MW)	28.2976	28.2573	26.5033	23.9558	27.5029	26.5747
$P_{G13}$ (MW)	25.0556	26.3754	26.5783	27.9007	21.8246	22.2063
$V_{G1}$ (p.u.)	1.0977	1.0133	1.1000	1.0995	1.0862	1.1000
$V_{G2}$ (p.u.)	1.0722	0.9980	1.0927	1.0906	1.0724	1.0881
$V_{G5}$ (p.u.)	1.0438	0.9582	1.0742	1.0686	1.0484	1.0718
$V_{G8}$ (p.u.)	1.0506	0.9844	1.0824	1.0747	1.0552	1.0767
$V_{G11}$ (p.u.)	1.0041	1.0942	1.1000	1.0919	1.0839	1.0938
$V_{G13}$ (p.u.)	1.1000	1.0020	1.0638	1.0891	1.0726	1.0951
$T_{11}$ (p.u.)	1.0833	1.0256	0.9639	1.0470	1.0433	1.0304
$T_{12}$ (p.u.)	0.9276	0.9492	1.0343	0.9146	0.9439	0.9469
$T_{13}$ (p.u.)	0.9719	0.9244	0.9781	1.0020	1.0061	1.0078
$T_{36}$ (p.u.)	0.9673	0.9459	1.0150	0.9697	0.9810	0.9818
$Q_{C10}$ (p.u.)	0.0480	0.0411	0.0386	0.0241	0.0293	0.0489
$Q_{C12}$ (p.u.)	0.0000	0.0469	0.0192	0.0248	0.0467	0.0314
$Q_{C15}$ (p.u.)	0.0500	0.0177	0.0178	0.0355	0.0460	0.0324
$Q_{C17}$ (p.u.)	0.0500	0.0241	0.0321	0.0286	0.0411	0.0460
$Q_{C20}$ (p.u.)	0.0314	0.0299	0.0324	0.0500	0.0490	0.0265
$Q_{C21}$ (p.u.)	0.0500	0.0452	0.0338	0.0455	0.0352	0.0249
$Q_{C23}$ (p.u.)	0.0414	0.0133	0.0311	0.0500	0.0121	0.0421
$Q_{C24}$ (p.u.)	0.0500	0.0452	0.0323	0.0289	0.0266	0.0424
$Q_{C29}$ (p.u.)	0.0057	0.0148	0.0437	0.0218	0.0011	0.0457
$Ob_p$ (MW)	-	-	-	5.1354	5.1599	<b>5.0796</b>
$Ob_v$ (ton/h)	0.2332	0.2350	<b>0.2329</b>	-	-	-
$Ob_f$ (\$/h)	833.5200	834.5679	<b>833.0155</b>	833.4465	835.4439	<b>832.3203</b>

TABLE 6. Comparison results of Case1.

algorithms	$Ob_f$ (\$/h)	$Ob_v$ (ton/h)
NSGA-II	0.2350	834.5679
DE-PFA	0.2332	833.5200
HFBA-COFS	0.2329	833.0155
AGSO [34]	0.2539	843.5473
MOEA/D [35]	0.2438	833.72
BSA [36]	0.2425	835.0199
ESDE [37]	0.2540	833.4743
ESDE-EC [37]	0.2510	831.0943
ESDE-MC [37]	0.2483	830.7185
MOPSO [12]	0.2492	833.7139
MODFA [12]	0.2432	831.6652

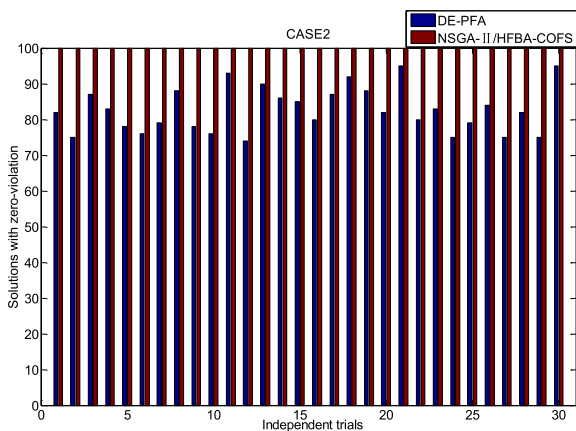


FIGURE 7. The numbers of feasible solutions for case2.

solutions. Besides, Table 5 provides the control variables of BCS solutions and it illustrates that the BCS of HFBA-COFS algorithm with 5.0796 MW of  $Ob_p$  and 832.3203 \$/h of

$Ob_f$  dominates the BCS solutions of DE-PFA and NSGA-II approaches. Furthermore, the comparison results of case2 are summarized in Table 7.

Above all, the proposed HFBA-COFS algorithm is superior to DE-PFA in obtaining more feasible solutions and has better performance than NSGA-II in seeking high-quality PFs and BCS solutions.

### 3) CASE3: $Ob_p$ and $Ob_f$

The performance of HFBA-COFS algorithm in optimizing the power loss and the fuel cost with value-points is studied in case3.

Figure 8 shows the PFs of case3 and it can be clearly seen that HFBA-COFS algorithm achieves the preferable PF while NSGA-II algorithm obtains the worse one. The numbers of feasible solutions for 30 independent trials obtained by three different algorithms are given in Figure 9.

TABLE 7. Comparison results of Case2.

algorithms	$Ob_p$ (MW)	$Ob_f$ (\$/h)
NSGA-II	5.1599	835.4439
DE-PFA	5.1354	833.4465
HFBA-COFS	5.0796	832.3203
MOEA/D [35]	4.9099	835.36
NSGA-II [35]	5.199	833.57
NSGA-III [12]	5.1775	836.8076
MODFA [12]	4.9561	833.9365

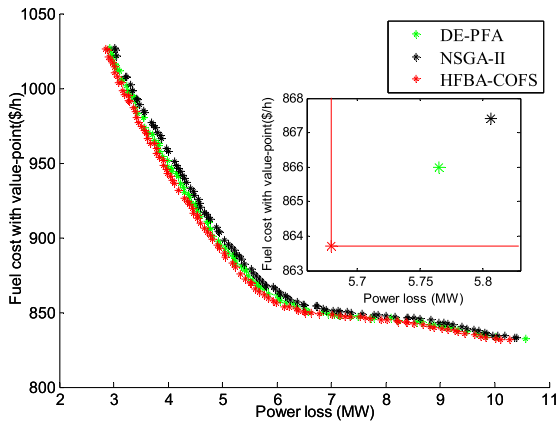


FIGURE 8. PFs of case3.

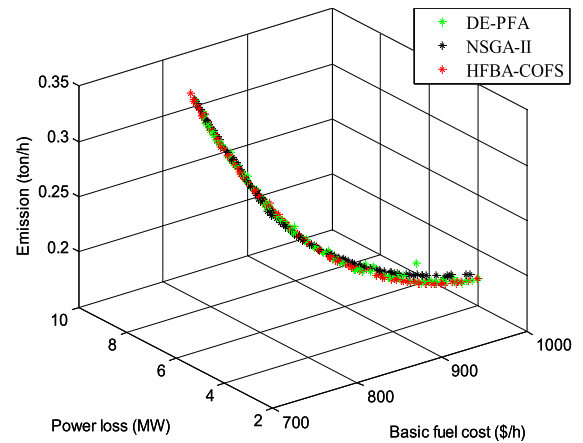


FIGURE 10. PFs of case4.

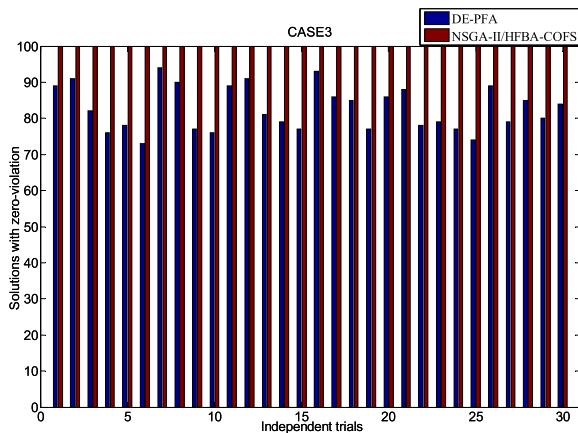


FIGURE 9. The numbers of feasible solutions for case3.

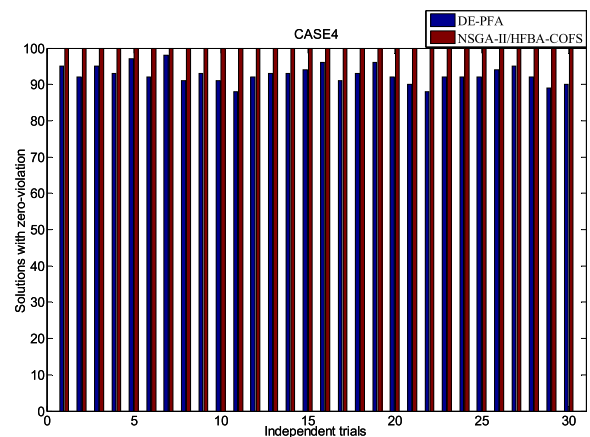


FIGURE 11. The numbers of feasible solutions for case4.

Meanwhile, Table 8 shows the control variables of three BCS solutions and two boundary solutions (BS). In detail, the BCS of HFBA-COFS algorithm with 5.6791 MW of  $Ob_p$  and 863.7107 \$/h of  $Ob_{fv}$  dominates the BCS solutions of two comparison algorithms. For two BS solutions obtained by HFBA-COFS algorithm, the  $BS_{case3-p}$  solution includes 1026.6437 \$/h of  $Ob_{fv}$  and 2.8461 MW of minimal  $Ob_p$  while the  $BS_{case3-fv}$  solution includes 10.2682 MW of  $Ob_p$  and 831.3694 \$/h of minimal  $Ob_{fv}$ . In a word, the HFBA-COFS algorithm can not only ensure that each solution of POS satisfies all equality and inequality constraints, but also be able to obtain the satisfactory PF.

#### 4) CASE4: $Ob_E$ , $Ob_p$ AND $Ob_f$

The tri-objective optimization with greater difficulty can further measure the effectiveness of HFBA-COFS algorithm. A synchronous optimization trial including  $Ob_e$ ,  $Ob_p$  and  $Ob_f$  is carried out on the IEEE 30-bus system in case4. Figure 10 gives the obtained PFs and it intuitively illustrates that the DE-PFA method obtains a relatively densely-distributed PF. In contrast to the NSGA-II algorithm, the HFBA-COFS algorithm is capable to achieve a higher-quality PF.

The numbers of feasible solutions for case4 is shown in Figure 11. Figure 11 indicates that the HFBA-COFS

TABLE 8. The control variables of BCS and BS solutions for case3.

variables	DE-PFA	NSGA-II	HFBA-COFS	BS <sub>case3-p</sub>	BS <sub>case3-fv</sub>
P <sub>G2</sub> (MW)	49.8503	43.8480	47.6172	80.0000	46.1045
P <sub>G5</sub> (MW)	30.7227	31.7346	31.6380	50.0000	18.0487
P <sub>G8</sub> (MW)	35.0000	34.6339	33.1641	35.0000	10.0000
P <sub>G11</sub> (MW)	24.9182	24.5906	23.2110	30.0000	10.0000
P <sub>G13</sub> (MW)	16.3338	20.0813	18.9426	40.0000	12.0000
V <sub>G1</sub> (p.u.)	1.1000	1.0786	1.1000	1.1000	1.1000
V <sub>G2</sub> (p.u.)	1.0895	1.0628	1.0898	1.0983	1.0850
V <sub>G5</sub> (p.u.)	1.0506	1.0473	1.0693	1.0799	1.0683
V <sub>G8</sub> (p.u.)	1.0683	1.0481	1.0767	1.0877	1.0637
V <sub>G11</sub> (p.u.)	1.0918	1.0962	1.0980	1.0964	1.0990
V <sub>G13</sub> (p.u.)	1.0710	1.0994	1.0999	1.1000	1.1000
T <sub>11</sub> (p.u.)	1.0813	1.0010	1.0008	1.0674	1.0265
T <sub>12</sub> (p.u.)	0.9000	0.9087	0.9672	0.9000	0.9113
T <sub>15</sub> (p.u.)	1.0030	0.9705	0.9782	0.9963	0.9909
T <sub>36</sub> (p.u.)	0.9507	0.9550	0.9643	0.9759	0.9423
Q <sub>C10</sub> (p.u.)	0.0366	0.0079	0.0367	0.0500	0.0424
Q <sub>C12</sub> (p.u.)	0.0359	0.0357	0.0232	0.0500	0.0000
Q <sub>C15</sub> (p.u.)	0.0369	0.0424	0.0180	0.0456	0.0028
Q <sub>C17</sub> (p.u.)	0.0256	0.0399	0.0467	0.0500	0.0482
Q <sub>C20</sub> (p.u.)	0.0248	0.0405	0.0492	0.0500	0.0408
Q <sub>C21</sub> (p.u.)	0.0500	0.0400	0.0494	0.0500	0.0493
Q <sub>C23</sub> (p.u.)	0.0500	0.0329	0.0463	0.0500	0.0020
Q <sub>C24</sub> (p.u.)	0.0136	0.0413	0.0386	0.0411	0.0449
Q <sub>C29</sub> (p.u.)	0.0126	0.0353	0.0216	0.0118	0.0047
Ob <sub>p</sub> (MW)	5.7655	5.8063	<b>5.6791</b>	<b>2.8461</b>	10.2682
Ob <sub>f</sub> (\$/h)	865.9950	867.4109	<b>863.7107</b>	1026.6437	<b>831.3694</b>

TABLE 9. The Control variables of BCS solutions for Case4 and Case5.

variables	case4			case5		
	DE-PFA	NSGA-II	HFBA-COFS	DE-PFA	NSGA-II	HFBA-COFS
P <sub>G2</sub> (MW)	63.6998	67.4691	64.2797	64.4637	64.4640	66.2056
P <sub>G5</sub> (MW)	33.4222	28.8768	34.9168	26.8692	31.4121	31.2893
P <sub>G8</sub> (MW)	35.0000	34.7962	35.0000	35.0000	34.7902	35.0000
P <sub>G11</sub> (MW)	30.0000	29.8874	30.0000	30.0000	27.2242	24.8720
P <sub>G13</sub> (MW)	35.1635	35.6755	31.7022	29.8510	28.4055	29.5606
V <sub>G1</sub> (p.u.)	1.1000	1.0285	1.1000	1.0985	1.0820	1.1000
V <sub>G2</sub> (p.u.)	1.0980	1.0155	1.0955	1.0917	1.0640	1.0900
V <sub>G5</sub> (p.u.)	1.0810	0.9999	1.0765	1.0658	1.0206	1.0573
V <sub>G8</sub> (p.u.)	1.0771	0.9989	1.0798	1.0459	1.0432	1.0753
V <sub>G11</sub> (p.u.)	1.0619	1.0765	1.0900	1.1000	1.0081	1.1000
V <sub>G13</sub> (p.u.)	1.0951	1.0718	1.0926	1.0794	1.0491	1.1000
T <sub>11</sub> (p.u.)	1.0568	0.9712	0.9756	1.0463	1.0042	0.9942
T <sub>12</sub> (p.u.)	0.9000	0.9374	1.0089	0.9871	0.9474	0.9374
T <sub>15</sub> (p.u.)	0.9650	0.9736	0.9787	0.9322	0.9925	0.9767
T <sub>36</sub> (p.u.)	0.9738	0.9213	0.9961	0.9616	0.9738	0.9838
Q <sub>C10</sub> (p.u.)	0.0276	0.0173	0.0500	0.0500	0.0163	0.0478
Q <sub>C12</sub> (p.u.)	0.0368	0.0136	0.0382	0.0200	0.0363	0.0362
Q <sub>C15</sub> (p.u.)	0.0258	0.0243	0.0338	0.0209	0.0238	0.0320
Q <sub>C17</sub> (p.u.)	0.0500	0.0340	0.0392	0.0500	0.0324	0.0289
Q <sub>C20</sub> (p.u.)	0.0343	0.0224	0.0331	0.0000	0.0004	0.0469
Q <sub>C21</sub> (p.u.)	0.0208	0.0339	0.0327	0.0000	0.0241	0.0500
Q <sub>C23</sub> (p.u.)	0.0318	0.0158	0.0122	0.0500	0.0205	0.0000
Q <sub>C24</sub> (p.u.)	0.0473	0.0216	0.0500	0.0172	0.0060	0.0500
Q <sub>C29</sub> (p.u.)	0.0376	0.0388	0.0336	0.0001	0.0493	0.0109
Ob <sub>p</sub> (MW)	4.2429	5.0865	<b>4.1544</b>	5.3973	5.2441	<b>4.6793</b>
Ob <sub>e</sub> (ton/h)	0.2087	0.2111	<b>0.2100</b>	0.2201	0.2198	<b>0.2195</b>
Ob <sub>f</sub> (\$/h)	-	-	-	919.0940	920.3811	<b>918.9154</b>
Ob <sub>f</sub> (\$/h)	869.9216	867.9027	<b>867.4262</b>	-	-	-

algorithm can achieve zero constraint-contravention even in the tri-objective optimization. Besides, the control variables of obtained BCS are listed in Table 9. It can be clearly known that the BCS obtained by HFBA-COFS algorithm which includes 4.1544 MW of  $Ob_p$ , 0.2100 ton/h of  $Ob_e$  and 867.4262 \$/h of  $Ob_f$  can dominate the BCS obtained by

NSGA-II algorithm with 5.0865 MW of  $Ob_p$ , 0.2111 ton/h of  $Ob_e$  and 867.9027 \$/h of  $Ob_f$ .

5) CASE5:OB<sub>E</sub>, OB<sub>P</sub> AND OB<sub>FV</sub>

In case5, three objectives including  $Ob_e$ ,  $Ob_p$  and  $Ob_{fv}$  are optimized simultaneously. Figure 12 and Figure 13 show the

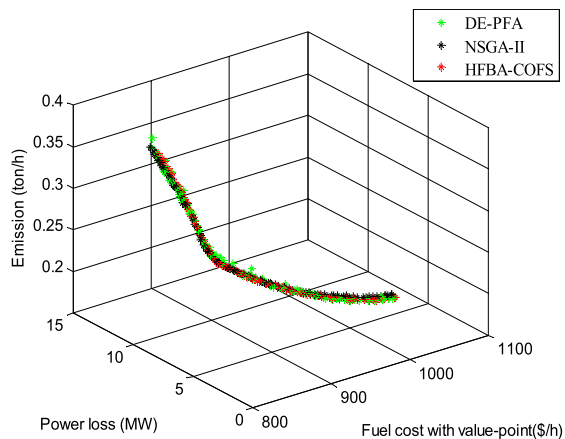


FIGURE 12. PFs of case5.

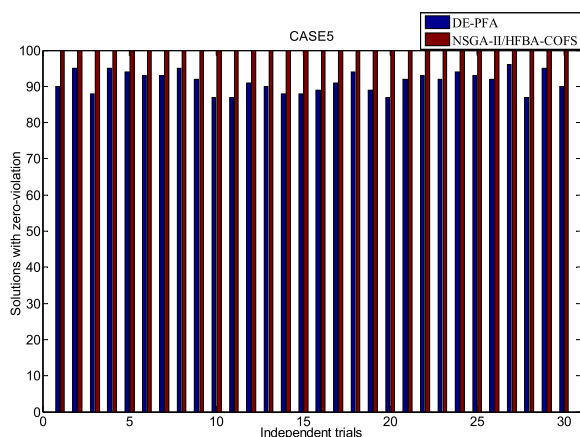


FIGURE 13. The numbers of feasible solutions for case5.

PFs of three mentioned algorithms and the numbers of feasible solutions, respectively. It is not difficult to find that the HFBA-COFS and NSGA-II algorithms can obtain relatively well-distributed PFs and achieve zero violation of system restrictions. Furthermore, Table 9 gives the detail information of BCS solutions. It illustrates that the BCS of HFBA-COFS algorithm with 4.6793 MW of  $Ob_p$ , 0.2195 ton/h of  $Ob_e$  and 918.9154 \$/h of  $Ob_f$ , is more preferable than the two BCS solutions of DE-PFA and NSGA-II approaches.

**D. TRIALS ON IEEE 57-BUS SYSTEM**

Two bi-objective and a tri-objective MOOPF trials are implemented on the IEEE 57-bus system. The complex structure of IEEE 57-bus system undoubtedly increases the optimization difficulty.

1) CASE6:  $OB_E$  and  $OB_f$

The optimization quality of proposed HFBA-COFS algorithm in minimizing emission and fuel cost on the IEEE 57-bus system is studied in case6. Figure 14 shows the PFs of three involved algorithms and the distribution of BCS solutions. It is easy to find that three intelligent algorithms can obtain evenly-distributed PFs while the HFBA-COFS

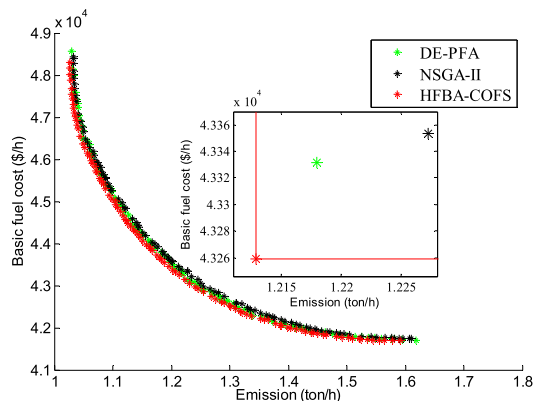


FIGURE 14. PFs of case6.

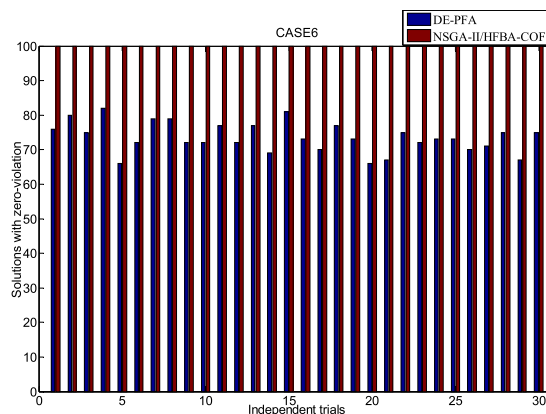


FIGURE 15. The numbers of feasible solutions for case6.

algorithm achieves the best one. Figure 15 shows the numbers of feasible solutions and it directly illustrates that compared with IEEE 30-bus system, the complex structure of IEEE 57-bus greatly limits the effectiveness of PFA method.

Table 10 gives the control variables of three BCS and two BS solutions for case6. The comparison result is listed in Table 10 as well. In detail, the BCS obtained by HFBA-COFS algorithm with 1.2129 ton/h of  $Ob_e$  and 43259.3013 \$/h of  $Ob_f$  dominates the BCS solutions obtained by two comparison algorithms. For the BS solutions determined by presented HFBA-COFS algorithm, the BS<sub>case6-e</sub> solution includes 1.0266 ton/h of minimal  $Ob_e$  and 48300.8388 \$/h of  $Ob_f$  while the BS<sub>case6-f</sub> solution includes 1.5910 ton/h of  $Ob_e$  and 41691.9581 \$/h of minimal  $Ob_f$ .

In a word, although the HFBA-COFS and NSGA-II methods enable each solution of obtained POS to satisfy all system constraints, the HFBA-COFS algorithm can obtain more advantageous PFs and higher-quality BCS solutions.

2) CASE7:  $OB_E$ ,  $OB_p$  AND  $OB_f$

A tri-objective optimization which takes  $Ob_e$ ,  $Ob_p$  and  $Ob_f$  into consideration concurrently is simulated on the IEEE 57-bus system. Figure 16 and Figure 17 show the obtained

TABLE 10. The control variables of BCS and BS solutions for Case6.

variables	DE-PFA	NSGA-II	HFBA-COFS	BS <sub>case6-e</sub>	BS <sub>case6-f</sub>	MODFA [12]
P <sub>G2</sub> (MW)	100.0000	98.8632	100.0000	100.0000	99.9995	99.9703
P <sub>G3</sub> (MW)	100.3757	96.9815	95.9347	140.0000	44.0060	88.2975
P <sub>G6</sub> (MW)	99.3326	99.0915	100.0000	100.0000	99.9995	99.9135
P <sub>G8</sub> (MW)	362.5321	362.2229	353.8717	270.3802	438.0784	343.6324
P <sub>G9</sub> (MW)	100.0000	99.9999	100.0000	100.0000	99.9995	99.9138
P <sub>G12</sub> (MW)	292.8837	294.6767	297.8883	235.9915	346.8237	310.8878
V <sub>G1</sub> (p.u.)	1.0561	1.0437	1.1000	1.1000	1.1000	1.0600
V <sub>G2</sub> (p.u.)	1.0450	1.0368	1.0999	1.1000	1.0994	1.0544
V <sub>G3</sub> (p.u.)	1.0599	1.0321	1.0966	1.0966	1.0949	1.0467
V <sub>G6</sub> (p.u.)	1.0841	1.0436	1.1000	1.1000	1.1000	1.0500
V <sub>G8</sub> (p.u.)	1.0943	1.0554	1.1000	1.1000	1.1000	1.0558
V <sub>G9</sub> (p.u.)	1.0551	1.0437	1.1000	1.1000	1.1000	1.0433
V <sub>G12</sub> (p.u.)	1.0345	1.0361	1.1000	1.1000	1.1000	1.0332
T <sub>19</sub> (p.u.)	1.0240	0.9726	1.1000	1.1000	1.1000	0.9916
T <sub>20</sub> (p.u.)	1.1000	1.0205	1.0886	1.0845	1.0959	0.9805
T <sub>31</sub> (p.u.)	1.1000	0.9361	1.0980	1.0971	1.0872	0.9972
T <sub>35</sub> (p.u.)	0.9778	0.9377	0.9571	0.9391	1.0107	0.9693
T <sub>36</sub> (p.u.)	1.0685	0.9467	1.0728	1.0788	1.0800	0.9646
T <sub>37</sub> (p.u.)	1.0565	1.0129	1.1000	1.1000	1.1000	0.9788
T <sub>41</sub> (p.u.)	0.9872	1.0016	1.1000	1.0864	1.0732	0.9570
T <sub>46</sub> (p.u.)	1.0428	0.9999	0.9286	0.9490	0.9716	0.9741
T <sub>54</sub> (p.u.)	0.9319	1.0627	0.9431	0.9473	0.9284	1.0310
T <sub>58</sub> (p.u.)	0.9501	0.9217	0.9889	0.9872	0.9942	0.9523
T <sub>59</sub> (p.u.)	0.9232	0.9644	0.9855	0.9707	0.9765	0.9452
T <sub>65</sub> (p.u.)	0.9639	0.9212	1.0015	0.9981	0.9970	1.0045
T <sub>66</sub> (p.u.)	0.9215	1.0433	0.9568	0.9631	0.9541	0.9344
T <sub>71</sub> (p.u.)	0.9814	0.9290	0.9932	1.0181	0.9910	0.9481
T <sub>73</sub> (p.u.)	1.0374	0.9774	0.9712	1.0234	0.9982	0.9621
T <sub>76</sub> (p.u.)	1.1000	0.9885	0.9175	0.9571	0.9926	0.9587
T <sub>80</sub> (p.u.)	0.9666	1.0367	1.0978	1.0924	1.0806	0.9703
Q <sub>C18</sub> (p.u.)	0.2524	0.0687	0.2637	0.2850	0.2835	0.1896
Q <sub>C25</sub> (p.u.)	0.1504	0.1376	0.1316	0.1251	0.1448	0.1191
Q <sub>C53</sub> (p.u.)	0.0242	0.0980	0.3000	0.3000	0.3000	0.0331
Ob <sub>e</sub> (ton/h)	1.2180	1.2272	<b>1.2129</b>	<b>1.0266</b>	1.5910	1.2679
Ob <sub>f</sub> (\$/h)	43331.7568	43353.5661	<b>43259.3013</b>	48300.8388	<b>41691.9581</b>	43174.5740

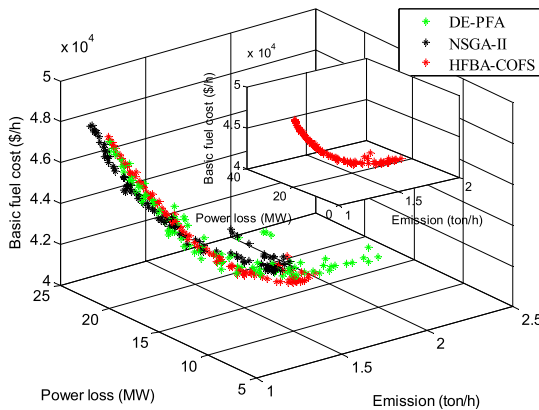


FIGURE 16. PFs of case7.

PFs and the numbers of feasible solutions, respectively. Figure 16 indicates the PFs obtained by DE-PFA and NSGA-II methods are distributed unevenly. It is clearly can be seen that only half of Pareto solutions obtained by DE-PFA algorithm can realize zero constraints-violation, which exposes the deficiency of PFA method. Moreover, Table 11 gives the details of BCS solutions achieved by three different algorithms. The BCS of HFBA-COFS algorithm

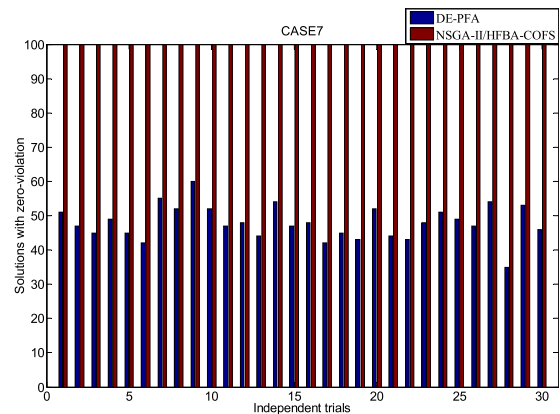


FIGURE 17. The numbers of feasible solutions for case7.

which is composed by 42856.4896 \$/h of  $Ob_f$ , 1.3436 ton/h of  $Ob_e$  and 11.5782 MW of  $Ob_p$  is more superior to the BCS of NSGA-II methods.

3) CASE8:  $OB_p$  AND  $OB_f$

In case8, a simulation trial which aims to optimize the  $Ob_p$  and  $Ob_f$  is carried out on the IEEE 57-bus system.

TABLE 11. The control variables of BCS solutions for Case7 and Case8.

variables	case7			case8	
	DE-PFA	NSGA-II	HFBA-COFS	NSGA-II	HFBA-COFS
$P_{G2}(MW)$	98.0996	95.6900	88.7933	56.3658	44.4742
$P_{G3}(MW)$	82.6023	89.8245	93.9957	62.8870	61.4752
$P_{G6}(MW)$	80.9479	89.5849	96.3316	94.8466	96.4101
$P_{G8}(MW)$	356.1245	317.5415	333.4141	369.9889	373.5684
$P_{G9}(MW)$	99.4656	99.8826	99.9650	99.3952	99.7557
$P_{G12}(MW)$	400.1520	407.8712	363.6433	408.5653	409.6130
$V_{G1}(p.u.)$	1.1000	1.0749	1.1000	1.0679	1.1000
$V_{G2}(p.u.)$	1.0909	1.0655	1.0997	1.0627	1.0973
$V_{G3}(p.u.)$	1.0940	1.0491	1.0995	1.0564	1.0983
$V_{G6}(p.u.)$	1.1000	1.0385	1.0998	1.0594	1.1000
$V_{G8}(p.u.)$	1.0898	1.0270	1.0999	1.0555	1.1000
$V_{G9}(p.u.)$	1.0893	1.0263	1.0775	1.0497	1.1000
$V_{G12}(p.u.)$	1.0867	1.0483	1.0702	1.0453	1.1000
$T_{19}(p.u.)$	1.0721	1.0039	1.0953	0.9127	1.0616
$T_{20}(p.u.)$	1.0974	1.0652	0.9759	1.0949	1.0626
$T_{31}(p.u.)$	1.0513	0.9914	0.9914	1.0449	1.0528
$T_{35}(p.u.)$	1.0181	1.0945	1.0893	0.9567	1.0987
$T_{36}(p.u.)$	1.1000	0.9125	0.9734	1.0305	1.0765
$T_{37}(p.u.)$	1.0248	1.0021	1.0250	1.0632	1.0174
$T_{41}(p.u.)$	1.0285	0.9747	1.0358	1.0053	1.0075
$T_{46}(p.u.)$	0.9550	0.9473	0.9170	0.9870	0.9925
$T_{54}(p.u.)$	0.9579	0.9005	0.9247	1.0529	0.9280
$T_{58}(p.u.)$	1.0286	0.9941	0.9796	0.9622	0.9790
$T_{59}(p.u.)$	1.0041	0.9716	0.9788	0.9504	1.0022
$T_{65}(p.u.)$	0.9874	1.0012	0.9771	0.9417	0.9878
$T_{66}(p.u.)$	0.9469	0.9739	0.9573	0.9214	0.9919
$T_{71}(p.u.)$	1.0340	0.9603	0.9874	0.9350	1.0547
$T_{73}(p.u.)$	0.9477	1.0147	1.0397	1.0506	1.1000
$T_{76}(p.u.)$	0.9516	0.9240	0.9147	0.9876	0.9824
$T_{80}(p.u.)$	1.0447	0.9929	1.0140	0.9894	1.0340
$Q_{C18}(p.u.)$	0.2160	0.2110	0.1112	0.0499	0.2338
$Q_{C25}(p.u.)$	0.1622	0.1805	0.1452	0.1309	0.1930
$Q_{C53}(p.u.)$	0.1966	0.1928	0.1573	0.1685	0.1491
$Ob_f$ (\$/h)	42387.1559	42887.0244	<b>42856.4896</b>	42125.6042	<b>42122.0140</b>
$Ob_c$ (ton/h)	1.5175	1.4572	<b>1.3436</b>	-	-
$Ob_p$ (MW)	11.3076	11.6865	<b>11.5782</b>	11.1296	<b>10.6995</b>

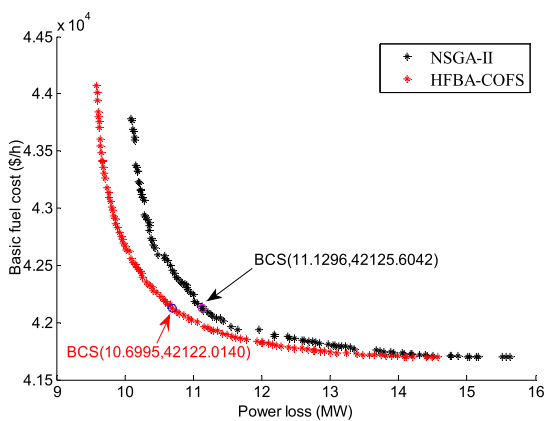


FIGURE 18. PFs of case8.

Figure 18 shows the PFs and two BCS solutions obtained by NSGA-II and HFBA-COFS algorithms. It clearly indicates that the PF of HFBA-COFS is significantly superior to that of NSGA-II method. It is worthy of note that since most of the solutions found by DE-PFA algorithm cannot satisfy all system constraints, the corresponding PF is not given in Figure 18. Table 11 also shows the control variables of

BCS solutions for case8. In great detail, the BCS obtained by HFBA-COFS algorithm including 42122.0140 \$/h of  $Ob_f$  and 10.6995 MW of  $Ob_p$  dominates the one obtained by NSGA-II method which is composed by 42125.6042 \$/h of  $Ob_f$  and 11.1296 MW of  $Ob_p$ .

### E. TRIALS ON IEEE 118-BUS SYSTEM

The complex structure of large-scale IEEE 118-bus system greatly limits the effectiveness of DE-PFA method. Both bi-objective and tri-objective cases are studied by NSGA-II and HFBA-COFS algorithm on the IEEE 118-bus system. So far, few algorithms have achieved satisfactory performance in solving MOOPF problems of IEEE 118-bus systems, which highlights the superiority of proposed HFBA-COFS method.

#### 1) CASE9: $Ob_p$ and $Ob_f$

The  $Ob_p$  and  $Ob_f$  are taken into consideration at the same time in case9. The PFs and BCS solutions obtained by HFBA-COFS and NSGA-II algorithms are shown in Figure 19. It can be intuitively seen that the PF of NSGA-II algorithm is much more densely-distributed than that of HFBA-COFS algorithm. Although the BCS found by

TABLE 12. The BCS and BS solutions of Case9 and Case10.

	case9				case10	
	BCS of NSGA-II	BCS of HFBA-COFS	BS <sub>case9-f</sub>	BS <sub>case9-p</sub>	BCS of NSGA-II	BCS of HFBA-COFS
$Ob_e$ (ton/h)	-	-	-	-	3.2475	<b>3.2085</b>
$Ob_p$ (MW)	58.8192	<b>61.0362</b>	73.9282	<b>54.8413</b>	89.7597	<b>63.7672</b>
$Ob_f$ (\$/h)	59900.3741	<b>59624.0613</b>	<b>59103.0835</b>	61002.6445	62002.9504	<b>61072.2077</b>

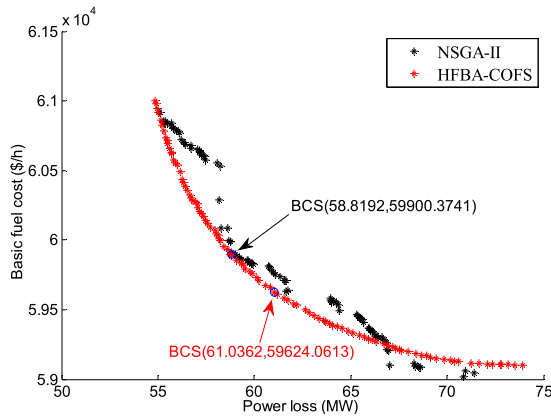


FIGURE 19. PFs of case 9.

HFBA-COFS algorithm which includes 61.0362 MW of  $Ob_p$  and 59624.0613 \$/h of  $Ob_f$  cannot dominate the BCS found by NSGA-II method, the PF of HFBA-COFS algorithm undoubtedly overmatches the PF of NSGA-II approach. Furthermore, the BCS solution of two involved algorithms and the BS solutions obtained by HFBA-COFS method are listed in Table 12. The BS<sub>case9-f</sub> represents the boundary solution with minimal  $Ob_f$  of 59103.0835 \$/h and the BS<sub>case9-p</sub> represents the boundary solution with minimal  $Ob_p$  of 54.8413MW.

2) CASE10:  $Ob_p$ ,  $Ob_e$  and  $Ob_f$

A tri-objective case which aims to minimize  $Ob_p$ ,  $Ob_e$  and  $Ob_f$  simultaneously is studied on the IEEE 118-bus system. Figure 20 shows the obtained PFs and the details of two BCS solutions. It is not difficult to find that the suggested HFBA-COFS algorithm achieves the satisfactory PF with relatively well-distribution. Table 12 also gives the two BCS solutions of case10 and it indicates the BCS found by HFBA-COFS algorithm with 3.2085 ton/h of  $Ob_e$ , 63.7672 MW of  $Ob_p$  and 61072.2077 \$/h of  $Ob_f$  is more advantageous than the BCS found by NSGA-II approach with 3.2475 ton/h of  $Ob_e$ , 89.7597 MW of  $Ob_p$  and 62002.9504 \$/h of  $Ob_f$ .

VI. PERFORMANCE ANALYSIS

The performance of HFBA-COFS algorithm in solving MOOPF problems is evaluated exhaustively from the following six aspects.

A. FEASIBLE SOLUTIONS

It is no doubt that the appropriateness of penalty coefficients is critical to the effectiveness of PFA approach. The enormous

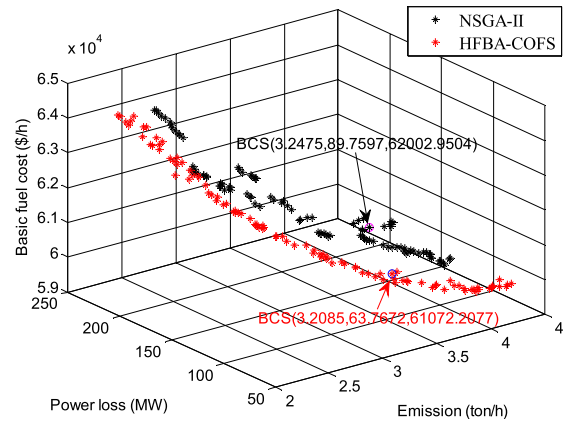


FIGURE 20. PFs of case 10.

difficulty in determining an appropriate penalty coefficient makes it almost impossible to realize the zero constraint-violation of each solution from obtained POS. Based on the numbers of feasible solutions for case1~ case7, the huge advantages of NSGA-II and HFBA-COFS algorithms which adopts the proposed CPR dominant strategy can be demonstrated. The CPR strategy effectively overcomes the defects of PFA method. More importantly, the obvious advantages of HFBA-COFS algorithm are more fully reflected on the large-scale power systems such as IEEE 57-bus and IEEE 118-bus systems.

B. DOMINANCE RATE OF BCS SOLUTIONS

From the perspective of dominance rate, the superiorities of HFBA-COFS algorithm in exploring higher-performance BCS solutions are verified. Table 13 gives the dominant relationships of HFBA-COFS algorithm in contrast to the DE-PFA and NSGA-II algorithms. It intuitively points out that the HFBA-COFS algorithm dominates the DE-PFA algorithm with a probability of 71.43% and dominates the NSGA-II algorithm with a probability of 90.00%.

C. PERFORMANCE METRICS

Two evaluation indicators, known as generational distance (GD) and SPREAD, are used to measure the consistency with the real PF, the distribution and diversity of obtained POS. Taking the three bi-objective optimization trials (case1~case3) carried out on the IEEE 30-bus system as examples, the optimization performance of three related algorithms based on the following two indexes is studied.

TABLE 13. The dominant relationships of HFBA-COFS algorithm.

algorithm	case1	case2	case3	case4	case5	case6	case7	case8	case9	case10	ratio%
DE-PFA	✓	✓	✓	✗	✓	✓	✗	-	-	-	71.43%
NSGA-II	✓	✓	✓	✓	✓	✓	✓	✓	✗	✓	90.00%

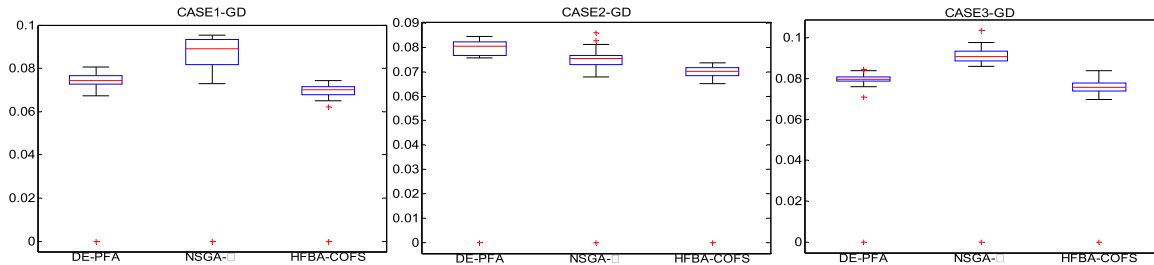


FIGURE 21. Boxplots of GD index for case1~case3.

TABLE 14. The mean and standard deviation values of two evaluation criteria.

metrics		SPREAD		GD	
		mean	deviation	mean	deviation
case1	DE-PFA	0.8657	<b>0.0114</b>	0.0722	0.0140
	NSGA-II	0.8804	0.0125	0.0848	0.0172
	HFBA-COFS	<b>0.8636</b>	0.0124	<b>0.0675</b>	<b>0.0130</b>
case2	DE-PFA	0.8539	<b>0.0118</b>	0.0774	0.0148
	NSGA-II	0.8663	0.0143	0.0730	0.0143
	HFBA-COFS	<b>0.8529</b>	0.0122	<b>0.0678</b>	<b>0.0130</b>
case3	DE-PFA	0.8512	0.0142	0.0772	0.0148
	NSGA-II	0.8740	0.0141	0.0854	0.0235
	HFBA-COFS	<b>0.8465</b>	<b>0.0117</b>	<b>0.0735</b>	<b>0.0142</b>

1) GD INDEX

The GD index defined as (40) is able to measure the distance between the obtained PF and the real one [12], [38]–[40]. The detail significance of relevant parameters is shown in literatures [7], [12]. In general, a smaller value of GD criterion indicates a better convergence to the real PF.

$$GD = \sqrt{\frac{\sum_{i=1}^T de_i^2}{T}} \quad (40)$$

In order to make a detail analysis about the GD and SPREAD indicators based on the average, standard deviation and outliers, the boxplot technique is adopted in this paper.

The boxplots of GD criterion for case1~case3 are shown in Figure 21. The mean and deviation values of DE-PFA, NSGA-II and HFBA-COFS algorithms are listed in Table 14. It is not difficult to find that the suggested HFBA-COFS algorithm achieves the smallest average and deviation values of GD indexes in all bi-objective trials on IEEE 30-bus system. It powerfully states that the PF obtained by HFBA-COFS algorithm has more favorable convergence and is more consistent with the true PF.

2) SPREAD INDEX

The SPREAD index defined as (41) is able to measure the extent of spread archived among the non-inferior solutions [41], [42]. The SPREAD=0 states that all obtained solutions are spaced equidistantly.

$$SPREAD = \frac{D_f + D_l + \sum_{i=1}^{T-1} |D_i - D_{avg}|}{D_f + D_l + (T - 1)D_{avg}} \quad (41)$$

where  $D_i$  is the Euclidean distance between the neighboring solutions and  $D_{avg}$  is the average of all  $D_i$ . The  $D_f$  and  $D_l$  are the Euclidean distances between the extreme solutions and the boundary ones.

For MOOPF problems, a smaller value of SPREAD criterion represents the preferable distribution and diversity of POS. The boxplots of SPREAD indicator for case1~case3 are shown in Figure 22 while the mean and deviation values are summarized in Table 14 as well. Although the HFBA-COFS algorithm has a relatively poor performance on the deviation values of SPREAD index, it still achieves the minimum mean values in case1~case3. It clearly states that the HFBA-COFS algorithm obtains the satisfactory POS with well-distribution and better-diversity.



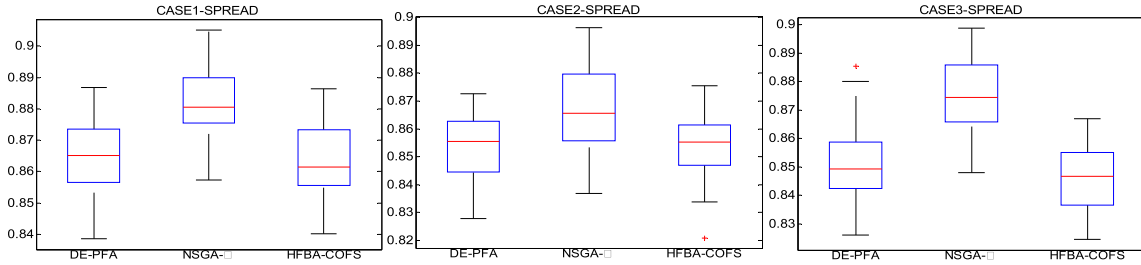


FIGURE 22. Boxplots of SPREAD index for case1~case3.

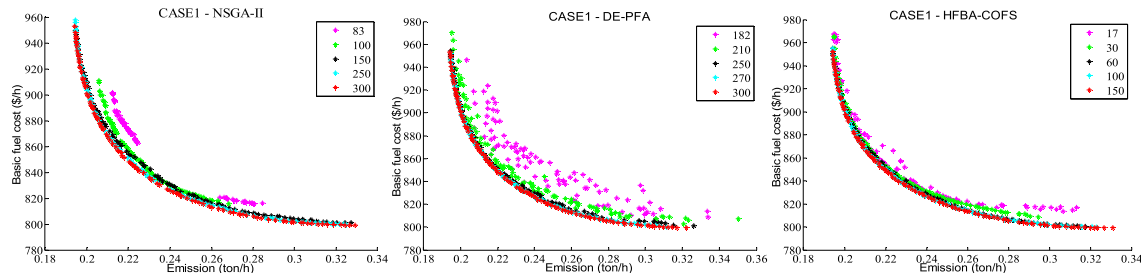


FIGURE 23. Iterative process of three algorithms for case1.

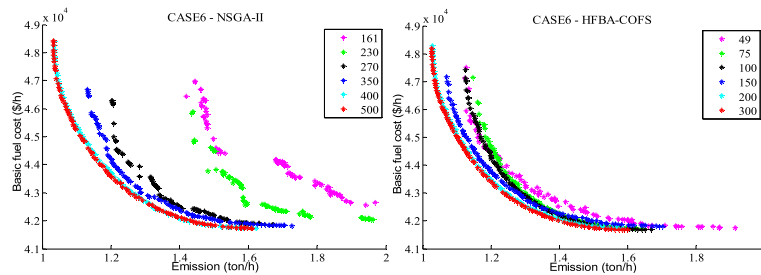


FIGURE 24. Iterative process of NSGA-II and HFBA-COFS algorithms for case6.

**D. CONVERGENCE ANALYSIS**

Two bi-objective MOOPF cases (case1 and case6), which are carried out on the IEEE 30-bus and IEEE 57-bus systems respectively, are used to prove the superiority of HFBA-COFS algorithm in fast-convergence. The convergence analysis for these MOOPF cases of IEEE 118-bus system is not carried out because the DE-PFA and NSGA-II methods cannot obtain the uniformly-distributed PFs with zero constraints-violation.

Figure 23 gives the PFs in iteration process of three mentioned methods for case1. The NSGA-II, DE-PFA and HFBA-COFS algorithms achieve zero constraints-violation at the 83th, 182th and 17th (with  $ite_{FA-max} = 50$ ) iterations, respectively. In addition, Figure 23 clearly indicates that the presented HFBA-COFS algorithm can converge to the most ideal PF around the 60th iteration while two comparison algorithms converge to the best PFs after at least 250th iterations.

Besides, Figure 24 gives the PFs in iteration process of case6. The DE-PFA method cannot guarantee that each solution of final POS set satisfies all system constraints, so its iterative convergence process is not given in Figure 24.

In complex IEEE 57-bus system, the NSGA-II and HFBA-COFS methods obtain qualified PFs at the 161th and 49th (with  $ite_{FA-max} = 100$ ) iterations, respectively. It also shows that the proposed HFBA-COFS algorithm can converge to the most ideal PF around the 200th iteration while the NSGA-II method converges to the best one around the 400th iteration.

Consequently, the suggested HFBA-COFS algorithm is provided with fast-convergence characteristics and great strength in seeking better-performance PFs with evenly-distribution and extensive-diversity.

**E. COMPUTATIONAL COMPLEXITY**

The mean CPU time of program running, as a common criterion to measure the computational complexity of intelligent algorithms, is summarized in Table 15. Table 15 intuitively shows that the HFBA-COFS algorithm requires more CPU time due to the unique local searching operation in contrast to the DE-PFA and NSGA-II methods. Therefore, improving the search efficiency is the key to the further optimization of bat algorithm.

**TABLE 15.** The mean CPU time (sec) of Ten simulation cases.

algorithm	case1	case2	case3	case4	case5	case6	case7	case8	case9	case10
DE-PFA	196.87	197.33	208.76	314.36	324.61	514.19	525.87	-	-	-
NSGA-II	196.10	205.45	207.32	313.81	318.43	504.04	519.10	510.17	1744	1765
HFBA-COFS	200.64	210.18	216.52	326.45	337.07	528.25	537.68	546.46	1759	1798

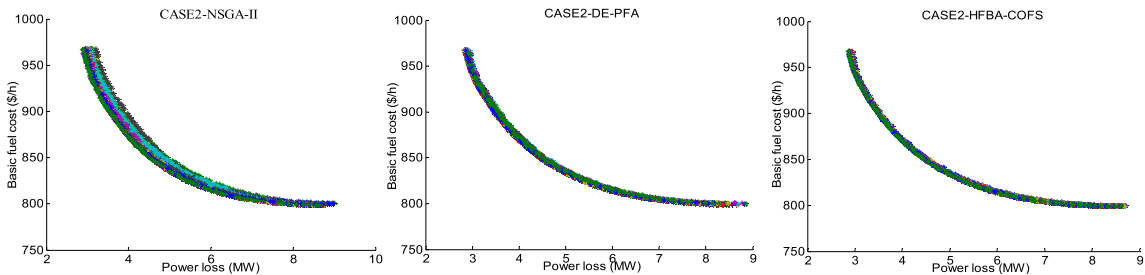


**FIGURE 25.** Superposition PFs of case2.

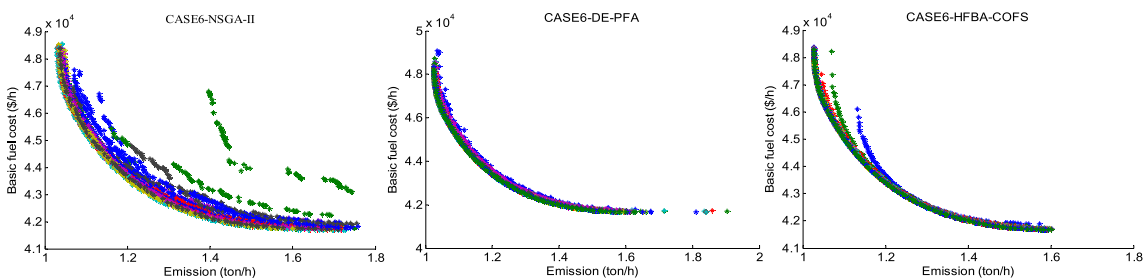


**FIGURE 26.** Superposition PFs of case6.

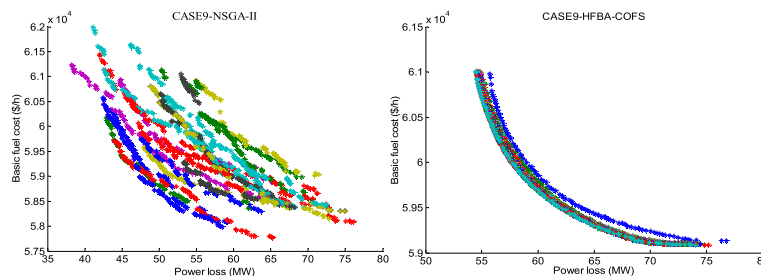


**FIGURE 27.** Superposition PFs of case9.

**F. SUPERPOSITION PFS**

Three bi-objective optimization cases, which are carried out different scale systems, are used as typical examples to analyze the superposition results of 30 independent trials. Figure 25 gives the superposition PFs of case2 which is simulated on the IEEE 30-bus system while Figure 26 gives the ones of case6 which is implemented on the IEEE 57-bus system. It clearly states that DE-PFA algorithm obtains more advantageous PFs in contrast to NSGA-II method while HFBA-COFS algorithm achieves the best PFs with better consistency. Figure 27 shows the superposition PFs of case9 which is carried out on the complex IEEE 118-bus system. It intuitively indicates that the HFBA-COFS

algorithm still achieves the well-distributed PFs of each separate trial while the superposition results of NSGA-II algorithm are much more unevenly.

The superposition PFs, which give the comprehensive results of thirty independent experiments, forcefully demonstrates the operation stability and superior quality of proposed HFBA-COFS algorithm especially on the large-scale IEEE 57-bus and 118-bus systems.

**VII. CONCLUSION**

In general, three main contributions are put forward in this paper to deal with the multi-dimensional and non-convex MOOPF problems.

1) The basic bat algorithm is modified by nonlinear weight coefficient and novel MRFM model. Combined with the MODFA algorithm for preliminary optimization, the proposed HFBA algorithm has more superior accuracy and excellent global-exploration ability.

2) The suggested CPR rule overcomes the difficulty of determining appropriate penalty coefficients.

3) Different from the typical sorting method, the presented COFS strategy provides an innovative and effective way to find the uniformly-distributed POS without any constraint-violation.

Compared with DE-PFA and NSGA-II methods, the HFBA-COFS algorithm has extensive applicability and great advantages in solving the complex MOOPF problems. In detail, a) HFBA-COFS algorithm realizes zero constraint-violation of all determined non-inferior solutions, which clearly overmatches the DE-PFA algorithm. b) HFBA-COFS algorithm is superior to NSGA-II method in seeking uniformly-distributed PFs and more ideal BCS solutions. c) HFBA-COFS algorithm is capable to handle both bi-objective and tri-objective MOOPF trials, even on the IEEE 118-bus system. The competitive edges of proposed HFBA-COFS method in obtaining the desirable POS with satisfactory-diversity and well-distribution are validated based on the evaluation metrics and superposition PFs.

Consequently, the HFBA-COFS algorithm provides a valid way to handle the non-linear MOOPF problems, which is highly significant to the safe and economical operation of power systems.

## REFERENCES

- [1] S. Duman, "A modified moth swarm algorithm based on an arithmetic crossover for constrained optimization and optimal power flow problems," *IEEE Access*, vol. 6, pp. 45394–45416, 2018.
- [2] E. Grover-Silva, M. Heleno, S. Mashayekh, G. Cardoso, R. Girard, and G. Kariniotakis, "A stochastic optimal power flow for scheduling flexible resources in microgrids operation," *Appl. Energy*, vol. 229, pp. 201–208, Nov. 2018.
- [3] E. E. Elattar and S. K. ElSayed, "Modified JAYA algorithm for optimal power flow incorporating renewable energy sources considering the cost, emission, power loss and voltage profile improvement," *Energy*, vol. 178, pp. 598–609, Dec. 2018.
- [4] Z. Ullah, S. Wang, J. Radosavljević, and J. Lai, "A solution to the optimal power flow problem considering WT and PV generation," *IEEE Access*, vol. 7, pp. 46763–46772, 2019.
- [5] W. Warid, H. Hizam, N. Mariun, and N. I. A. Wahab, "A novel quasi-oppositional modified Jaya algorithm for multi-objective optimal power flow solution," *Appl. Soft Comput.*, vol. 65, pp. 360–373, Apr. 2018.
- [6] S. Rahmani and N. Amjady, "Improved normalised normal constraint method to solve multi-objective optimal power flow problem," *IET Gener., Transmiss. Distrib.*, vol. 12, no. 4, pp. 859–872, Feb. 2018.
- [7] G. Chen, J. Qian, Z. Zhang, and Z. Sun, "Applications of novel hybrid bat algorithm with constrained Pareto fuzzy dominant rule on multi-objective optimal power flow problems," *IEEE Access*, vol. 7, pp. 52060–52084, 2019.
- [8] H. Liang, Y. Liu, F. Li, and Y. Shen, "A multiobjective hybrid bat algorithm for combined economic/emission dispatch," *Int. J. Elect. Power Energy Syst.*, vol. 101, pp. 103–115, Oct. 2018.
- [9] S. S. Reddy, "Solution of multi-objective optimal power flow using efficient meta-heuristic algorithm," *Elect. Eng.*, vol. 100, no. 2, pp. 401–413, Jun. 2018.
- [10] X. Yuan, B. Zhang, P. Wang, J. Liang, Y. Yuan, Y. Huang, and X. Lei, "Multi-objective optimal power flow based on improved strength Pareto evolutionary algorithm," *Energy*, vol. 122, pp. 70–82, Mar. 2017.
- [11] E. Barocio, J. Regalado, E. Cuevas, F. Uribe, P. Zúñiga, and P. J. R. Torres, "Modified bio-inspired optimisation algorithm with a centroid decision making approach for solving a multi-objective optimal power flow problem," *IET Gener., Transmiss. Distrib.*, vol. 11, no. 4, pp. 1012–1022, Mar. 2017.
- [12] G. Chen, X. Yi, Z. Zhang, and H. Wang, "Applications of multi-objective dimension-based firefly algorithm to optimize the power losses, emission, and cost in power systems," *Appl. Soft Comput.*, vol. 68, pp. 322–342, Jul. 2018.
- [13] C. K. Ng, C. H. Wu, W. H. Ip, and K. L. Yung, "A smart bat algorithm for wireless sensor network deployment in 3-D environment," *IEEE Commun. Lett.*, vol. 22, no. 10, pp. 2120–2123, Oct. 2018.
- [14] Y. Lu and T. Jiang, "Bi-population based discrete bat algorithm for the low-carbon job shop scheduling problem," *IEEE Access*, vol. 7, pp. 14513–14522, 2019.
- [15] H. Liang, Y. Liu, Y. Shen, F. Li, and Y. Man, "A hybrid bat algorithm for economic dispatch with random wind power," *IEEE Trans. Power Syst.*, vol. 33, no. 5, pp. 5052–5061, Sep. 2018.
- [16] R. Murugan, M. R. Mohan, C. C. A. Rajan, P. D. Sundari, and S. Arunachalam, "Hybridizing bat algorithm with artificial bee colony for combined heat and power economic dispatch," *Appl. Soft Comput.*, vol. 72, pp. 189–217, Nov. 2018.
- [17] Y. Yuan, X. Wu, P. Wang, and X. Yuan, "Application of improved bat algorithm in optimal power flow problem," *Appl. Intell.*, vol. 48, no. 8, pp. 2304–2314, Aug. 2018.
- [18] G. Xiong and D. Shi, "Hybrid biogeography-based optimization with brain storm optimization for non-convex dynamic economic dispatch with valve-point effects," *Energy*, vol. 157, pp. 424–435, May 2019.
- [19] G. Chen, X. Yi, Z. Zhang, and H. Lei, "Solving the multi-objective optimal power flow problem using the multi-objective firefly algorithm with a constraints-prior Pareto-domination approach," *Energies*, vol. 11, no. 12, p. 3438, Dec. 2018.
- [20] T. Ding, R. Bo, F. Li, Y. Gu, Q. Guo, and H. Sun, "Exact penalty function based constraint relaxation method for optimal power flow considering wind generation uncertainty," *IEEE Trans. Power Syst.*, vol. 30, no. 3, pp. 1546–1547, May 2015.
- [21] J. Qiao, H. Zhou, C. Yang, and S. Yang, "A decomposition-based multiobjective evolutionary algorithm with angle-based adaptive penalty," *Appl. Soft Comput.*, vol. 74, pp. 190–205, Jan. 2019.
- [22] K. Deb, A. Pratap, S. Agarwal, and T. Meyarivan, "A fast and elitist multiobjective genetic algorithm: NSGA-II," *IEEE Trans. Evol. Comput.*, vol. 2, no. 6, pp. 182–197, Apr. 2002.
- [23] J.-H. Yi, S. Deb, J. Dong, A. H. Alavi, and G.-G. Wang, "An improved NSGA-III algorithm with adaptive mutation operator for big data optimization problems," *Future Gener. Comput. Syst.*, vol. 88, pp. 571–585, Nov. 2018.
- [24] P. C. Roy, K. Deb, and M. M. Islam, "An efficient nondominated sorting algorithm for large number of fronts," *IEEE Trans. Cybern.*, vol. 49, no. 3, pp. 859–869, Mar. 2019.
- [25] M. A. Al-Betar, M. A. Awadallah, H. Faris, X.-S. Yang, A. T. Khader, and O. A. Alomari, "Bat-inspired algorithms with natural selection mechanisms for global optimization," *Neurocomputing*, vol. 273, pp. 448–465, Jan. 2018.
- [26] E. Osaba, X.-S. Yang, I. Fister, Jr., J. Del Ser, P. Lopez-Garcia, and A. J. Vazquez-Pardavila, "A discrete and improved bat algorithm for solving a medical goods distribution problem with pharmacological waste collection," *Swarm Evol. Comput.*, vol. 44, pp. 273–286, Feb. 2019.
- [27] H. Zhang and Q. Hui, "Many objective cooperative bat searching algorithm," *Appl. Soft Comput.*, vol. 77, pp. 412–437, Apr. 2019.
- [28] J. Huang, X. Chen, and D. Wu, "A switch-mode firefly algorithm for global optimization," *IEEE Access*, vol. 6, pp. 54177–54184, 2018.
- [29] H.-C. Huang and S.-K. Lin, "A hybrid metaheuristic embedded system for intelligent vehicles using hypermutated firefly algorithm optimized radial basis function neural network," *IEEE Trans. Ind. Informat.*, vol. 15, no. 2, pp. 1062–1069, Feb. 2019.
- [30] Y. Yang, B. Wei, H. Liu, Y. Zhang, J. Zhao, and E. Manla, "Chaos firefly algorithm with self-adaptation mutation mechanism for solving large-scale economic dispatch with valve-point effects and multiple fuel options," *IEEE Access*, vol. 6, pp. 45907–45922, 2018.
- [31] A.-A. A. Mohamed, Y. S. Mohamed, A. A. M. El-Gaafary, and A. M. Hemeida, "Optimal power flow using moth swarm algorithm," *Electr. Power Syst. Res.*, vol. 142, pp. 190–206, Jan. 2017.

- [32] G. Chen, S. Qiu, Z. Zhang, Z. Sun, and H. Liao, "Optimal power flow using Gbest-guided cuckoo search algorithm with feedback control strategy and constraint domination rule," *Math. Problems Eng.*, vol. 2, Dec. 2017, Art. no. 9067520.
- [33] M. Ghasemi, S. Ghavidel, M. M. Ghanbarian, and M. Gitizadeh, "Multi-objective optimal electric power planning in the power system using Gaussian bare-bones imperialist competitive algorithm," *Inf. Sci.*, vol. 294, pp. 286–304, Feb. 2015.
- [34] N. Daryani, M. T. Hagh, and S. Teimourzadeh, "Adaptive group search optimization algorithm for multi-objective optimal power flow problem," *Appl. Soft Comput.*, vol. 38, pp. 1012–1024, Jan. 2016.
- [35] J. Zhang, Q. Tang, P. Li, D. Deng, and Y. Chen, "A modified MOEA/D approach to the solution of multi-objective optimal power flow problem," *Appl. Soft Comput.*, vol. 47, pp. 494–514, Oct. 2016.
- [36] A. E. Chaib, H. R. E. H. Boucekara, R. Mehasni, and M. A. Abido, "Optimal power flow with emission and non-smooth cost functions using backtracking search optimization algorithm," *Int. J. Elect. Power Energy Syst.*, vol. 81, pp. 64–77, Oct. 2016.
- [37] H. Pulluri, R. Naresh, and V. Sharma, "An enhanced self-adaptive differential evolution based solution methodology for multiobjective optimal power flow," *Appl. Soft Comput.*, vol. 54, pp. 229–245, May 2017.
- [38] H. Ishibuchi, R. Imada, Y. Setoguchi, and Y. Nojima, "Reference point specification in inverted generational distance for triangular linear Pareto front," *IEEE Trans. Evol. Comput.*, vol. 22, no. 6, pp. 961–975, Dec. 2018.
- [39] R. Sengupta and S. Saha, "Reference point based archived many objective simulated annealing," *Inf. Sci.*, vol. 467, pp. 725–749, Oct. 2018.
- [40] H. Chen, G. Wu, W. Pedrycz, P. N. Suganthan, and X. Zhu, "An adaptive resource allocation strategy for objective space partition-based multiobjective optimization," *IEEE Trans. Syst., Man, Cybern., Syst.*, to be published.
- [41] F. S. Lobato, M. N. Sousa, M. A. Silva, and A. R. Machado, "Multi-objective optimization and bio-inspired methods applied to machinability of stainless steel," *Appl. Soft Comput.*, vol. 22, pp. 261–271, Sep. 2014.
- [42] G. Ruan, G. Yu, J. Zheng, J. Zou, and S. Yang, "The effect of diversity maintenance on prediction in dynamic multi-objective optimization," *Appl. Soft Comput.*, vol. 58, pp. 631–647, Sep. 2017.



**JIE QIAN** received the bachelor's degree in electrical engineering and automation from the Chongqing University of Posts and Telecommunications (CQUPT), Chongqing, China, in 2017, where she is currently pursuing the master's degree. Her research interests include optimal power flow and application of artificial intelligence in power systems.



**ZHIZHONG ZHANG** received the M.S. degree in communication network testing from the Chongqing University of Posts and Telecommunications, China, 1998, and the Ph.D. degree from the School of Communication Engineering, University of Electronic Science and Technology of China, in 2002. He is currently a Professor with the Chongqing University of Posts and Telecommunications, China. His research interests include mobile communication testing technology, broadband information networking, 5G networking, and optimal power flow in power systems.



**GONGGUI CHEN** received the B.S. degree in physics from Huazhong Normal University, the M.E. degree in computer technology, and the Ph.D. degree in electrical engineering from the Huazhong University of Science and Technology (HUST), China. He is currently a Professor with the Department of Electrical Engineering, College of Automation, Chongqing University of Posts and Telecommunications, Chongqing, China. His research interests include economic dispatch, optimal power flow, and application of artificial intelligence in power systems.



**ZHI SUN** received the B.E. degree in computer science and technology and the M.E. degree in electrical engineering from the Huazhong University of Science and Technology (HUST), China, in 2004 and 2012, respectively. He is currently an Electronic Engineering Engineer with Chn Energy Enshi Hydropower Company Ltd., China. His research interests include intelligent substation, economic dispatch, optimal power flow, and application of artificial intelligence in power systems.

• • •